This is a preprint, the final version is subject to change, of the American Mineralogist (MSA)
Cite as Authors (Year) Title. American Mineralogist, in press.
(DOI will not work until issue is live.) DOI: http://dx.doi.org/10.2138/am-2016-5665

Revision 2

Physical basis of trace element partitioning: A review

Shun-ichiro Karato

Yale University

Department of Geology and Geophysics

New Haven, CT 06520, USA

submitted to *American Mineralogist (Centennial Volume)*

revised April 22, 2016

key words: element partitioning, point defects, the Onuma diagram, strain energy model, hard sphere model, noble gas

This is a preprint, the final version is subject to change, of the American Mineralogist (MSA)
Cite as Authors (Year) Title. American Mineralogist, in press.
(DOI will not work until issue is live.) DOI: http://dx.doi.org/10.2138/am-2016-5665

Abstract

Experimental observations on the dissolution of elements in minerals and melts and the partitioning between the two materials show that the concentration (or the partition coefficient) of trace elements depends on the properties of elements as well as those of relevant materials (minerals and melts) and the thermochemical conditions. Previous models of element solubility in minerals contain a vague treatment of a role of the stiffness of the element and have a difficulty in explaining some observations including the solubility of the noble gases. A modified theory of element solubility in minerals is presented where the role of elasticity of both matrix mineral and the element is included using the continuum theory of point defects by Eshelby. This theory provides a framework to explain a majority of observations and shows a better fit to the published results on the effective elastic constants relevant to element partitioning. However, the concept of "elasticity of the trace element" needs major modifications when the site occupied by a trace element has large excess charge. The experimental data of the solubility coefficients of noble gases in the melts show strong dependence on the atomic size that invalidates the 'zero-charge' model for noble gas partitioning. A simple model of element solubility in the melts is proposed based on the hard sphere model of complex liquids that provides a plausible explanation for the difference in the dissolution behavior between noble gases and other charged elements. Several applications of these models are discussed including the nature of noble gas behavior in the deep/early Earth and the water distribution in the lithosphere/asthenosphere system.

This is a preprint, the final version is subject to change, of the American Mineralogist (MSA)
Cite as Authors (Year) Title. American Mineralogist, in press.
(DOI will not work until issue is live.) DOI: http://dx.doi.org/10.2138/am-2016-5665

INTRODUCTION

The distribution of elements in various materials on Earth has been used to infer the chemical evolution of Earth including the history of partial melting and degassing that has created the crust, atmosphere and oceans (e.g., (Allègre, 1982; Allègre et al., 1986/1987; Hofmann, 1997; Matsui et al., 1977)). The distribution of elements is controlled largely by the difference in the excess free energy of a given element in co-exiting materials (e.g., (Blundy and Wood, 2003; Matsui et al., 1977; Nagasawa, 1966)), although kinetic factors might also contribute if diffusion is slow (e.g., (Lee et al., 2007; Van Orman et al., 2002)). When we assume chemical equilibrium to simplify the discussion, then the element distribution is controlled by the differences in the excess free energy of elements in coexisting materials such as minerals and melts.

The concentration of trace elements in minerals and melts changes with the physical and chemical conditions as well as the properties of minerals (melts) and elements. Consequently, understanding the controlling factors of concentration of elements in minerals and melts will help us understand the physical and chemical processes in Earth. This is an area where mineralogists (mineral physicists) can make an important contribution to geochemistry.

Obviously, the most direct and crucial studies would be the experimental studies on element partitioning but experimental studies of partitioning (solubility [1]) are challenging and the data set is incomplete particularly under the deep Earth conditions. In some cases, there are large discrepancies among published results (e.g., a case of noble gas partition coefficients in olivine and clinopyroxene: (Broadhurst et al., 1992; Hiyagon

[1] I use the term "solubility" in a broad sense meaning the amount of an element in a material in the given thermo-chemical environment.

This is a preprint, the final version is subject to change, of the American Mineralogist (MSA)
Cite as Authors (Year) Title. American Mineralogist, in press.
(DOI will not work until issue is live.) DOI: http://dx.doi.org/10.2138/am-2016-5665

and Ozima, 1986)). In case of *Ar*, for example, even the issue of either *Ar* behaves like compatible or incompatible element upon partial melting (or solidification from the melt) is controversial (e.g., (Broadhurst et al., 1992; Shcheka and Keppler, 2012; Watson et al., 2007)). Understanding the theoretical basis for dissolution of elements will help assess the experimental observations.

In most of geochemical studies, we focus on the partitioning of *trace elements* (elements with small concentration) because they are believed to behave as a passive marker of physical/chemical processes (such as partial melting) without changing the nature of the processes themselves. In these cases, the essence of theory of solubility of trace elements in minerals is much the same as the theory of point defects in solids: both point defects and trace elements are "impurities" in nearly perfect crystals. Therefore, the results of a large amount of theoretical and experimental studies on point defects in solids (for review, see e.g., (Eshelby, 1956; Flynn, 1972)) can be used to help understand the physical mechanisms of element solubility (partitioning). In case of dissolution of trace elements in the complex liquids (melts), somewhat different models will apply since the structure and the thermodynamic properties of complex liquids are quite different from those of solids (e.g., (Barrat and Hansen, 2003; Jing and Karato, 2011)).

In this paper, I will first review the basic observations on element partitioning, summarize thermodynamics of element partitioning, and then discuss the physical models of element solubility (uptake) including previously published models (Blundy and Wood, 1994, 2003; Carroll and Stolper, 1993; Guillot and Sarda, 2006; Nagasawa, 1966). In the case of the solubility in solids, the previous models have a common limitation in explaining why different elements and minerals have different partitioning, the most

important goal of a theory. The limitation of the previous models becomes serious when one considers the solubility (partitioning) of noble gas elements that have unusually smaller "stiffness" than the host crystal. I will present a modified theory of element partitioning to rectify this and finally discuss some implications.

In case of the liquids (melts), some theoretical models were proposed to explain the solubility of noble gases (Carroll and Stolper, 1993; Guillot and Sarda, 2006). However, the applicability of these models to other trace elements is unknown. I will present a simple conceptual model of element dissolution in the melts based on the hard sphere model of complex liquids (e.g., (Guillot and Sarda, 2006; Jing and Karato, 2011)) and suggest that the dissolution mechanisms in the melts are different between neutral elements (noble gases) and charged elements: noble gas elements go to the void space while other charged trace elements replace an ion in the molecular cluster.

EXPERIMENTAL OBSERVATIONS ON ELEMENT PARTITIONING AND SOLUBILITY

The equilibrium distribution of an element between two materials can be characterized by a partition coefficient that describes the ratio of concentration of a given element between two materials. The concentration of an element can be defined in a few different ways, and therefore there are several definitions of the partition coefficient (e.g., (Blundy and Wood, 2003)). In most geochemical literatures, the concentration of an element is measured by the weight fraction (as oxides in many cases) and the Nernst partitioning coefficient is used that is defined by

This is a preprint, the final version is subject to change, of the American Mineralogist (MSA)
Cite as Authors (Year) Title. American Mineralogist, in press.
(DOI will not work until issue is live.) DOI: http://dx.doi.org/10.2138/am-2016-5665

$$\tilde{D}_i^{Y/X} = \frac{\tilde{C}_i^Y}{\tilde{C}_i^X} \quad (1)$$

where $\tilde{C}_i^{Y(X)}$ is the mass fraction of element *i* in phase *Y* (or *X*) (all the symbols used in this paper are summarized in **Table 1**). Instead of the mass fraction, the molar fraction may be used to define the molar partition coefficient,

$$D_i^{Y/X} = \frac{C_i^Y}{C_i^X} \quad (2)$$

where $C_i^{Y(X)}$ is the molar fraction of the element *i* in phase *Y* (or *X*). An alternative measure of element partitioning is the equilibrium constant,

$$K_i^{Y/X} = \frac{a_i^Y}{a_i^X} \quad (3)$$

where $a_i^{Y(X)}$ is the activity of element *i* in phase *Y*(*X*). Thermodynamically this is the simplest definition because $K_i^{Y/X}$ contains only the thermodynamic properties of pure end-member components. The molar partition coefficient, $D_i^{Y/X}$, is identical to the equilibrium constant when the activity of an element in a given material is the same as its

This is a preprint, the final version is subject to change, of the American Mineralogist (MSA)
Cite as Authors (Year) Title. American Mineralogist, in press.
(DOI will not work until issue is live.) DOI: http://dx.doi.org/10.2138/am-2016-5665

128 molar concentration (i.e., ideal solution). I will make this assumption for simplicity and
129 review the models for $D_i^{Y/X}$ (or $K_i^{Y/X}$)[2].

130 There is an extensive literature on element partitioning (for reviews, see (Blundy
131 and Wood, 2003; Jones, 1995; Wood and Blundy, 2004)). There are several features in
132 element partitioning (or solubility) that should be explained by a physical model:

133 (i) For a given pair of materials (say clinopyroxene and basaltic melt) at a given
134 physical/chemical condition, trace elements with different sizes and electric
135 charges have different partition coefficients (e.g., **Fig. 1a**, (Blundy and Dalton,
136 2000; Onuma et al., 1968)).

137 (ii) For a given element, partition coefficients depend strongly on minerals (and
138 sometimes on melts). An important case is the contrast between *Mg*-perovskite
139 and *Ca*-perovskite (e.g., **Fig. 1b, c**, (Corgne et al., 2004; Hirose et al., 2004)) and
140 between diopside and olivine (e.g., (Witt-Eickschen and O'Neill, 2005)).

141 (iii) Even for the same pair of materials, partition coefficient of some elements (say
142 hydrogen) depends strongly on thermo-chemical conditions such as temperature,
143 pressure and the fugacity of relevant species. A case is the hydrogen partitioning
144 between olivine and orthopyroxene (e.g., **Fig. 1d**, (Dai and Karato, 2009)).

145 (iv) The noble gas partition coefficient between olivine, diopside and the melt is
146 nearly independent of the size of noble gas atom (e.g., **Fig. 1e,** (Brooker et al.,
147 2003; Heber et al., 2007)) whereas the solubility of noble gas atom in bridgmanite
148 strongly depends on the atomic size (**Fig. 1f**, (Shcheka and Keppler, 2012)).

[2] There are a few important cases where this assumption is not valid. In these cases, the role of fugacity of relevant species is important.

This is a preprint, the final version is subject to change, of the American Mineralogist (MSA)
Cite as Authors (Year) Title. American Mineralogist, in press.
(DOI will not work until issue is live.) DOI: http://dx.doi.org/10.2138/am-2016-5665

(v) The solubility coefficient of noble gas in the melt is highly sensitive to the atomic size of the noble gas (e.g., **Fig. 1g,** (Carroll and Stolper, 1993; Heber et al., 2007; Shibata et al., 1998; Shibata et al., 1994)).

The issues listed as (i) through (iii) are all fundamental to the physics and chemistry of element partitioning, but previous models to explain these features are highly limited as I will discuss in the next section. For example, the influence of the properties of trace element on the partitioning was not properly formulated in the previous models. Also, the issue (iii), i.e., the sensitivity of the partition coefficient on physical and chemical conditions has not been fully appreciated. Although this is a consequence of a general physics and chemistry of element partitioning (see the next section), the element partition coefficient is often considered to be a constant rather than a property that depends on the physical/chemical conditions. Important cases are hydrogen partitioning between olivine and orthopyroxene (Dai and Karato, 2009) and the *H/Ce* ratios in basaltic magmas (Dixon et al., 2002) both of which have important ramifications to the study of distribution of water (hydrogen).

Solubility and partitioning of the noble gases require special attention. Understanding the behavior of noble gases is important because they provide important clues to the evolution of Earth and other terrestrial planets (e.g., (Allègre et al., 1983; Marty, 2012; Ozima, 1994)). Noble gas atoms have weak chemical bonding to other atoms and hence the free energy change caused by the dissolution of noble gas atoms into minerals and melts can be markedly different from those of other trace elements where charged trace elements (e.g., $H^+, La^{3+}, Sm^{3+}, U^{4+}$) replace other cations (e.g., $Mg^{2+}, Ca^{2+}, Al^{3+}, Si^{4+}$) in the host minerals or melts.

This is a preprint, the final version is subject to change, of the American Mineralogist (MSA)
Cite as Authors (Year) Title. American Mineralogist, in press.
(DOI will not work until issue is live.) DOI: http://dx.doi.org/10.2138/am-2016-5665

THEORETICAL MODELS FOR ELEMENT SOLUBILITY (PARTITIONING)

Chemical reactions and thermodynamics

Physics of element partitioning can be viewed in a few different ways. When one considers element partitioning between melt (liquid) and mineral (solid), one could imagine a model where a trace element *i* and host element *h* are exchanged between a liquid and a solid (**Fig. 2a**)[3], viz.,

$$S(y) + L(i) \Leftrightarrow S(i) + L(y) \quad (4)$$

where $S(y)$ is a solid (mineral) containing cation *y*, and $L(i)$ is a liquid (melt) containing element *i* etc. The free energy change associated with the reaction (4) can be calculated by dividing the reaction into two separate reactions (**Fig. 2a**), namely,

$$S(y) \rightarrow L(y) \quad (5a)$$

and

$$L(i) \rightarrow S(i). \quad (5b)$$

[3] In reality, there are several cases where the exchange of multiple elements is involved in the dissolution of some elements ("coupled substitution", e.g., $Al^{3+} + H^{+} \Leftrightarrow Si^{4+}$). To simplify the discussion, I will focus on simple cases (without coupled substitution), and will discuss the issues of coupled substitution only briefly in relation to hydrogen and noble gas partitioning.

This is a preprint, the final version is subject to change, of the American Mineralogist (MSA)
Cite as Authors (Year) Title. American Mineralogist, in press.
(DOI will not work until issue is live.) DOI: http://dx.doi.org/10.2138/am-2016-5665

192 The reaction (5a) is melting of the host mineral, and the free energy change
193 associated with this reaction is the free energy change upon melting (ΔG^{y}_{fusion} in the
194 notation by (Blundy and Wood, 1994)). The reaction (5b), $L(i) \rightarrow S(i)$, is a reaction to
195 bring a trace element from the liquid to the solid (the free energy change is $\Delta G^{y-i}_{exchange}$ in
196 (Blundy and Wood, 1994)). Blundy and Wood (1994) argued that the latter is dominated
197 by the strain energy in solid and developed a model using the theory by (Brice, 1975). In
198 this treatment, the role of liquid (melt) is obscured because the free energy change in the
199 liquid (melt) is included only *implicitly* in $\Delta G^{y-i}_{exchange}$. In fact, I will show that the role of
200 liquid is important in the case of noble gas where the dissolution of noble gas in the melt
201 has non-negligible excess free energy.
202 The physical nature of the change in the free energy associated with element
203 partitioning between a solid and a liquid can be understood more clearly by considering
204 the chemical reactions of both a solid (mineral) and a liquid (melt) with an "environment
205 (a reservoir)" that is a fluid phase (**Fig. 2b**). In this approach, I consider element
206 dissolution in a solid and a liquid separately, and by taking the ratio of the concentration
207 of a given element in a solid and a liquid, I will calculate the partition coefficient. The
208 chemical equilibrium of material *X* (either a solid or a liquid) with a reservoir *A* with
209 respect to the exchange of elements *i* and *y* can be written as
210
211 $$A(i; y-1) + X(i-1; y) = A(i-1; y) + X(i; y-1) \qquad (6)$$
212

This is a preprint, the final version is subject to change, of the American Mineralogist (MSA)
Cite as Authors (Year) Title. American Mineralogist, in press.
(DOI will not work until issue is live.) DOI: http://dx.doi.org/10.2138/am-2016-5665

where $A(i;y-1)$ is a reservoir containing the element *i* and *y*-1, $X(i;y-1)$ is a phase *X* that contains an element *i* as an impurity and the host cation *y-1*. Rewriting equation (6), one gets,

$$\tilde{A}(i;y) = \tilde{X}(i;y) \quad (7)$$

where $\tilde{A}(i;y) = A(i;y-1) - A(i-1;y)$ and $\tilde{X}(i;y) = X(i;y-1) - X(i-1;y)$. The chemical equilibrium of reaction (7) demands

$$\mu_{\tilde{A}(i;y)} = \mu_{\tilde{X}(i;y)} \quad (8)$$

where $\mu_{\tilde{A}(i;y)}$ is the chemical potential of the reservoir (*A*) containing element *i* and *y* and $\mu_{\tilde{X}(i;y)}$ is the chemical potential of phase *X* (solid or liquid) containing element *i* and *y*. I assume that the reservoir is large, and therefore the properties of the reservoir are insensitive to the amount of host element, i.e., $\mu_{\tilde{A}(i;y)} \approx \mu_{\tilde{A}(i)}$. Then

$$\mu_{\tilde{A}(i)} = \mu^{o}_{\tilde{A}(i)} + RT\, log \frac{f_{\tilde{A}(i)}}{P_o} \quad (9)$$

where $f_{\tilde{A}(i)}$ is the fugacity of element *i* in the reservoir $\tilde{A}(i)$, P_o is the reference pressure and $\mu^{o}_{\tilde{A}(i)}$ is the chemical potential of the reservoir at the reference pressure (and temperature).

This is a preprint, the final version is subject to change, of the American Mineralogist (MSA)
Cite as Authors (Year) Title. American Mineralogist, in press.
(DOI will not work until issue is live.) DOI: http://dx.doi.org/10.2138/am-2016-5665

As to the chemical potential of *X* (a solid or a liquid) containing some trace element, $\mu_{\tilde{X}(i;y)}$, I will assume that the amount of trace element is small and hence the change in the concentration of the host cation (say from *y* to *y-1*) does not change the chemical potential of the solid (or the liquid), $\mu_{\tilde{X}(i;y)} \approx \mu_{\tilde{X}(i)}$. This assumption also leads to an ideal solution model where the chemical potential of a solid (or a liquid) containing the trace element is given by,

$$\mu_{\tilde{X}(i)} = \mu^{0}_{\tilde{X}(i)} + RT\, log\, C_i^X \qquad (10)$$

where $\mu^{0}_{\tilde{X}(i)}$ is the change in chemical potential of phase *X* by replacing the host cation (*y*) with a trace element (*i*) (i.e., the formation free energy of a "defect"), C_i^X is the (molar) concentration of element *i* in a phase *X*, and *RT* has their usual meaning[4].

In writing the chemical equilibrium between the reservoir (a fluid phase) and a solid (or a liquid), it is necessary to know how many molecules of the fluid phase are involved in the given reaction. For instance, when *Ar* is dissolved in a mineral, one may write

$$Ar + X = X(Ar) \qquad (11)$$

where one mole of *Ar* reacts to form a mineral containing a certain amount of *Ar*. The situation is different in case of the dissolution of hydrogen *H* in a mineral. In this case,

[4] In a more realistic case, where trace elements interact each other, one needs to make a correction to the relation (8) by introducing the activity coefficient.

This is a preprint, the final version is subject to change, of the American Mineralogist (MSA)
Cite as Authors (Year) Title. American Mineralogist, in press.
(DOI will not work until issue is live.) DOI: http://dx.doi.org/10.2138/am-2016-5665

the above formula must be modified because hydrogen can react with other species such as oxygen *O* to form a "compound" such as OH or $(2H)_M^{\times}$ (two protons trapped at the M-site vacancy). In this case, we can write the chemical reaction equation as

$$\alpha \cdot H_2O + X = X(H) \qquad (12)$$

where α is a constant that depends on the nature of *H*-bearing chemical species contained in phase *X* such as *OH* or $(2H)_M^{\times}$ (two protons trapped at M-site). In case of *OH,* α=½, whereas in case of $(2H)_M^{\times}$, α=1 (e.g., (Karato, 2008)).

Therefore the concentration of element *i* in mineral *X* that co-exists with a reservoir for element *i* (a fluid phase A) is given by

$$C_i^{X,A} = exp\left(\frac{\alpha_i^X \mu^0_{\tilde{A}(i)}}{RT}\right) \cdot \left[\frac{f_{\tilde{A}(i)}(P,T)}{P_o}\right]^{\alpha_i^X} \cdot exp\left(-\frac{\mu^0_{\tilde{X}(i)}}{RT}\right). \qquad (13)$$

$C_i^{X,A}$ is the solubility of element *i* in mineral *X* if the fluid phase *A* is the end-member phase (e.g., if the fluid phase is water, then equation (13) will be the solubility of hydrogen (*i*) in mineral *X*). The same formula applies to another material (mineral or melt), *Y*. The ratio of concentration of a species *i* between two phases (*Y* and *X*) can then be given by

$$\frac{C_i^{Y,A}}{C_i^{X,A}} = D_i^{Y/X} = exp\left[\frac{\left(\alpha_i^X - \alpha_i^Y\right)\mu^o_{\tilde{A}(i)}}{RT}\right] \cdot f_{\tilde{A}(i)}^{\alpha_i^X - \alpha_i^Y}(P,T) \cdot exp\left(-\frac{\mu^0_{\tilde{Y}(i)} - \mu^0_{\tilde{X}(i)}}{RT}\right) \qquad (14)$$

This is a preprint, the final version is subject to change, of the American Mineralogist (MSA)
Cite as Authors (Year) Title. American Mineralogist, in press.
(DOI will not work until issue is live.) DOI: http://dx.doi.org/10.2138/am-2016-5665

where $\alpha_i^{Y(X)}$ are the coefficients in chemical reaction such as (11), $D_i^{Y/X}$ is the molar partition coefficient of an element *i* between the phase *Y* and *X*, that is equivalent to the molar partition coefficient if the ideal solution model works.

A simple but important and general conclusion from the relations (13) and (14) is that the partition coefficient is generally a function of thermodynamic conditions including pressure, temperature and the fugacity of relevant components. In other words, the tendency of an element to prefer one phase over another phases depends on the thermodynamic conditions. Consequently, experimental data on element partitioning obtained under some limited conditions should not be applied to largely different conditions without proper corrections. For instance, the partition coefficient of hydrogen between olivine and orthopyroxene changes with pressure, temperature and water fugacity by a large amount, say a factor of 10 or more ((Dai and Karato, 2009), see also (Sakurai et al., 2014)).

A case of trace element partitioning can be treated easily if one considers the partitioning of elements with similar chemical properties (e.g., partitioning of rare Earth elements). In such a case, one can assume $\alpha_i^X = \alpha_i^Y$, and the term containing the properties of the reservoir can be eliminated, and equation (14) becomes

$$\frac{C_i^{Y,A}}{C_i^{X,A}} = \frac{C_i^Y}{C_i^X} = exp\left(-\frac{\mu^0_{\tilde{Y}(i)} - \mu^0_{\tilde{X}(i)}}{RT}\right). \quad (15)$$

This is a preprint, the final version is subject to change, of the American Mineralogist (MSA)
Cite as Authors (Year) Title. American Mineralogist, in press.
(DOI will not work until issue is live.) DOI: http://dx.doi.org/10.2138/am-2016-5665

297 Consequently, in this case the only task is to evaluate how $\mu^0_{\tilde{Y}(i)} - \mu^0_{\tilde{X}(i)}$ depends on the
298 properties of the element and the matrix.

299 In the literatures, the element partitioning between the melts and minerals is
300 discussed (e.g., (Blundy and Wood, 2003; Matsui et al., 1977; Nagasawa, 1966; Onuma
301 et al., 1968; Wood and Blundy, 2004)). In these cases, although the influence of melt
302 composition is studied (e.g., (Blundy and Dalton, 2000; O'Neill and Eggins, 2002;
303 Schmidt et al., 2006)), it is often assumed that the excess energy for the melt is
304 independent of the trace element ($\mu^0_{\tilde{Y}(i)}$ is independent of trace element, *i*), and the
305 discussion is focused on the excess energy in minerals ($\mu^0_{\tilde{X}(i)}$). Noble gases are
306 exceptions: their solubility in melts is small and highly sensitive to the atomic size of the
307 noble gas, the solubility (coefficient) varies more than a factor of ~100 among different
308 species (e.g., (Carroll and Stolper, 1993; Heber et al., 2007; Shibata et al., 1998)). The
309 physical reasons for different behavior will be discussed in a later section based on the
310 hard sphere model of silicate melts.

311 When the role of melts is minor, then the main question is what determines the
312 different solubility of different elements in different minerals (what controls the degree of
313 "incompatibility")? One may ask two different questions: (1) why different elements
314 have different solubility in a given mineral?, and (2) why different minerals have
315 different solubility for a given element? Such questions were addressed by a pioneer of
316 geochemistry, Goldschmidt, who also classified elements into several categories based on
317 the affinity to various materials (Goldschmidt, 1937). Goldschmidt pointed out that the

This is a preprint, the final version is subject to change, of the American Mineralogist (MSA)
Cite as Authors (Year) Title. American Mineralogist, in press.
(DOI will not work until issue is live.) DOI: http://dx.doi.org/10.2138/am-2016-5665

size of ions and the crystal structure of minerals (as well as the charge of the ion) are the key to determine the partition coefficients[5].

The breakthrough on this topic was made by Onuma, Matsui and their colleagues (Matsui et al., 1977; Nagasawa, 1966; Onuma et al., 1968) who clearly showed that the partition coefficients of elements between minerals and melts depend on the size (ionic radius) of that element relative to the size of the site in the mineral as envisaged by Goldschmidt. A diagram showing the partition coefficients as a function of ionic radius is called the *Onuma diagram.*

Outline of the models for the excess free energy

The excess free energy associated with the dissolution of a trace element may be calculated from theoretical models incorporating the atomistic details (e.g., (Allan et al., 2001; Purton et al., 1996; Purton et al., 2000)), but the use of simpler theoretical models will make the basic physics clearer. Therefore, I will focus on the theoretical models from which some essence of element solubility can be understood.

Two types of models will be considered. In case of a solid (a mineral), the change in free energy caused by the dissolution of trace element is dominated by the change in enthalpy, i.e., the change in internal energy and volume. A trace element in a crystal can be considered as a *point defect*, and therefore the change in internal energy and volume associated with trace element dissolution may be formulated following the models of point defects (e.g., (Eshelby, 1954, 1956; Flynn, 1972; Mott and Littleton, 1938)).

[5] "One of the most important principles for the distribution of the elements is the grading according to their size, especially as compared with the lattice spacings or interatomic distances of rock-forming minerals" (from *Goldschmidt* (1937)).

This is a preprint, the final version is subject to change, of the American Mineralogist (MSA)
Cite as Authors (Year) Title. American Mineralogist, in press.
(DOI will not work until issue is live.) DOI: http://dx.doi.org/10.2138/am-2016-5665

The excess free energy caused by a point defect can be calculated by the response of a crystal to the introduction of a point defect. A point defect exerts some force to the surrounding crystal. This force could be separated into two components, the force caused by the "size" mismatch and the force caused by the excess charge. The first force causes uniform displacement of cations and anions, while the second one causes opposite displacement between cations and anions, i.e., the dielectric polarization. The excess free energy associated with the first can be expressed as the strain energy, while the latter as the electrostatic energy. In some cases, these two effects are related and I will come back to that point when I discuss the dissolution of noble gases. Although this is a gross simplification of the actual processes of formation of point defects (or the dissolution of trace elements), such an approach provides a good estimate of some properties of point defects in olivine and other minerals (e.g., (Karato, 1977, 1981; Lasaga, 1980)).

Dissolution of a trace element in complex liquids such as silicate melts should be treated in a different way because thermodynamic properties of complex liquids are markedly different from those of solids (minerals). The differences in thermodynamic properties include small (and a narrow range of) bulk moduli that are unrelated to the bulk moduli of corresponding solids and the positive pressure dependence of Grüneisen parameter. Jing and Karato (2011) showed that most of these observations can be explained by a hard-sphere model in which the main contribution to the free energy is the configurational entropy rather than the enthalpy. In this model, a silicate melt is considered to be a mixture of hard spheres and free space, and the motion of hard spheres in the free space contributes to the configurational entropy. A trace element could go either into the free space (void space) or into the hard spheres by replacing the pre-

This is a preprint, the final version is subject to change, of the American Mineralogist (MSA)
Cite as Authors (Year) Title. American Mineralogist, in press.
(DOI will not work until issue is live.) DOI: http://dx.doi.org/10.2138/am-2016-5665

existing ions in them. I will discuss these two cases based on the hard sphere model of a complex liquid in a later section.

Continuum models of excess energy for a solid

When an atom (or an ion) in a crystal is replaced with another one (I will call it as a trace element), the free energy of the crystal will change. The change in chemical potential (the Gibbs free energy per mole) is generally expressed as

$$\Delta\mu = \Delta u + P\Delta\upsilon - T\Delta s = \Delta h - T\Delta s \qquad (16)$$

where $\Delta\mu$ is a change in the chemical potential, Δu is a change in the internal energy, $\Delta\upsilon$ is a change in the volume, and Δs is a change in the entropy (Δh is a change in enthalpy). In solids, the entropy change in this equation corresponds to a change in the vibrational entropy (Flynn, 1972). In general a change in the vibrational entropy caused by a point defect is a fraction of R (measured by J/K/mol) (e.g., (Maradudin et al., 1971)), and the influence of this term on element partitioning is small ($exp\left(\frac{\Delta s}{R}\right) \approx O(1)$). The pressure effect $P\Delta\upsilon$ is important when partition coefficient under a broad pressure range is investigated. However, the emphasis in this paper is to provide a good explanation for the behavior of partition coefficient for different elements or for different materials (under the limited pressure (and temperature) conditions), so I will focus on Δu.

In contrast, in silicate melts, the change in configurational entropy can be large when a trace element atom occupies the "free space" (or the void space). This is likely

the case for the dissolution of noble gases in melts (e.g., (Carroll and Stolper, 1993; Guillot and Sarda, 2006)). In these cases, the entropy term cannot be ignored.

The trace element that replaces an ion in the host crystal has in general a different size and charge than those of the ion in the matrix that will be replaced with the trace element. Therefore the dissolution of a trace element creates excess elastic strain and dielectric polarization of a crystal (in addition to the change in the strain energy of the trace element itself). In the continuum approximation, the excess energy may be written as

$$\mu^{0}_{\bar{Y}(i)} = \mu^{elastic}_{\bar{Y}(i)} + \mu^{dielectric}_{\bar{Y}(i)} \tag{17}$$

where $\mu^{elastic}_{\bar{Y}(i)}$ is the excess elastic strain energy and $\mu^{dielectric}_{\bar{Y}(i)}$ is the excess dielectric polarization energy.

Under these approximations, the partition coefficient can be written as

$$\begin{aligned} D_i^{Y/X} &= D_i^{Y/X,elastic} \cdot D_i^{Y/X,dielectric} \\ &\approx exp\left(-\frac{\Delta u^{elastic}}{RT}\right) \cdot exp\left(-\frac{\Delta u^{dielectric}}{RT}\right) \end{aligned} \tag{18}$$

where $D_i^{Y/X,elastic} \approx exp\left(-\frac{\Delta u^{elastic}}{RT}\right)$, $D_i^{Y/X,dielectric} \approx exp\left(-\frac{\Delta u^{dielectric}}{RT}\right)$ and the quantities are for one mole, and the symbols *i*, *Y/X* are removed in the second line for simplicity.

Strain energy models

This is a preprint, the final version is subject to change, of the American Mineralogist (MSA)
Cite as Authors (Year) Title. American Mineralogist, in press.
(DOI will not work until issue is live.) DOI: http://dx.doi.org/10.2138/am-2016-5665

Now let us focus on the contribution from the elastic strain, $\Delta u^{elastic}$. The replacement of an ion with a trace element with a different size (r_o: the radius of the site at which a trace element is placed, r_1: the radius of the trace element) results in the excess elastic strain energy. The strain energy is determined by the magnitude of strain caused by this replacement and the elastic properties of both the matrix crystal and of the trace element. Therefore the key here is to calculate (i) the magnitude of strain and (ii) the strain energy associated with this process.

(Nagasawa, 1966) was the first to discuss the nature of trace element partitioning based on the strain energy model. He used a theory by (Eshelby, 1954) and calculated the strain energy associated with the dissolution of a trace element assuming that the elastic properties of the matrix crystal are the same as those of the trace element. This assumption is valid only when the bulk moduli (only bulk modulus matters inside the inclusion according to the theory of (Eshelby, 1954)) of the matrix and the trace element are the same. In a more general case, the influence of different elastic properties of the matrix and the trace element needs to be included. Also, Nagasawa (1966) ignored the influence of the image force (Eshelby, 1954, 1956) causing small differences in the formula for the effective elastic constant (see also **Table 2**).

Blundy and Wood (e.g., (Blundy and Wood, 1994, 2003; Wood and Blundy, 1997, 2001, 2004)) used a model by (Brice, 1975) to interpret a large number of experimental data including the partitioning of noble gases. Their model is similar to that by (Nagasawa, 1966), but the model by (Brice, 1975) contains a few physically unsound assumptions. For instance, Brice assumes that when a trace element with the radius r_1 is inserted to a site with the radius r_o, then the radius of the site changes to r_1. This is

This is a preprint, the final version is subject to change, of the American Mineralogist (MSA)
Cite as Authors (Year) Title. American Mineralogist, in press.
(DOI will not work until issue is live.) DOI: http://dx.doi.org/10.2138/am-2016-5665

428 correct only when the trace element is infinitely stiff. In a more general case where the
429 trace element has a finite bulk modulus, the displacement is not only controlled by the
430 size difference but also by the difference in the elastic constants. This leads to a large
431 systematic error when the trace element is much softer than the matrix, a case for the
432 noble gas. Furthermore, Brice used an incorrect expression for the strain both inside and
433 outside of the inclusion. The strain field in the matrix surrounding a spherical inclusion is
434 shear strain and the strain inside of the inclusion is compressional strain (Eshelby, 1956),
435 but Brice used a Young's modulus and did not pay attention to the difference in the strain
436 field inside and outside of an inclusion. Despite these differences, these two models give
437 similar equations (**Table 2**), and both of them explain some of the experimental
438 observations (e.g., the Onuma diagram for some elements).

439 In short, these previous models have common limitations in ignoring the
440 difference in the elastic properties between the matrix and the trace element (impurity).
441 An important case is the partitioning of noble gas elements where the trace element
442 (impurity) has much smaller bulk modulus than the matrix. In such a case, the strain
443 would be small $\varepsilon = \left| \frac{\bar{r}}{r_o} - 1 \right| \ll 1$ much less than the Brice model would predict $\varepsilon = \frac{r_1}{r_0} - 1$.

444 The appropriate treatment of the role of the size and stiffness of the trace element
445 is a key step in understanding how the properties of the trace elements and of the matrix
446 affect element partitioning. As will be shown later, the stiffness of the trace element has a
447 strong influence on the magnitude of lattice strain and therefore it is one of the key
448 parameters controlling the strain energy. To rectify the limitations of these previous
449 models, I have made modifications to the continuum model of trace element solubility by
450 introducing the following three points: (i) the proper boundary conditions at the boundary

This is a preprint, the final version is subject to change, of the American Mineralogist (MSA)
Cite as Authors (Year) Title. American Mineralogist, in press.
(DOI will not work until issue is live.) DOI: http://dx.doi.org/10.2138/am-2016-5665

451 between the inserted (trace) element and the surrounding matrix (i.e., the continuity of the
452 displacement and the normal stress) are included in solving the equation for the
453 equilibrium conditions (this was included in (Nagasawa, 1966) but not in (Brice, 1975)),
454 (ii) the strain energy of the element itself is included in addition to the strain energy of
455 the host crystal using the different elastic moduli (in previous models, strain energy in the
456 trace element was calculated assuming the same elastic constant as the matrix) and (iii)
457 both volumetric and shear strain are considered (this was correctly included in
458 (Nagasawa, 1966) but Brice used an incorrect relationship for the strain).

459 An analysis including these points shows that the displacement of the boundary
460 caused by the replacement of an atom (ion) with the radius r_o with that of a trace element
461 with the radius r_1 depends not only on the relative size but also on the elastic constants of
462 the trace element and of the matrix as (**Fig. 3;** see also **Appendix 1**)

463

464 $$\varepsilon = \frac{\tilde{r}}{r_o} - 1 = \frac{K_1}{K_1 + \frac{4}{3}G_o}\left(\frac{r_1}{r_o} - 1\right) \qquad (19)$$

465

466 where $\tilde{r}$ is the final (equilibrium) size of the site now occupied by a trace element, G_o is
467 the shear modulus of the matrix and K_1 is the "bulk modulus" of the trace element[6].
468 Equation (19) means that if the trace element is very stiff compared to the shear modulus
469 of the matrix ($K_1 \gg G_o$), then $\tilde{r} \approx r_1$, whereas for a weak trace element ($K_1 \ll G_o$),
470 $\tilde{r} \approx r_o$ (and $\varepsilon \approx 0$) (**Fig. 4**). This concept plays a key role in explaining the solubility
471 (partitioning) of noble gas elements. Corresponding to this displacement, both the

[6] Physical meaning of the bulk modulus of a trace element in a lattice site can be complicated and will be discussed in the later part of this paper.

This is a preprint, the final version is subject to change, of the American Mineralogist (MSA)
Cite as Authors (Year) Title. American Mineralogist, in press.
(DOI will not work until issue is live.) DOI: http://dx.doi.org/10.2138/am-2016-5665

element itself and the crystal will undergo elastic deformation leading to an increase in the strain energy (per one trace element) that is given by (**Appendix 1**),

$$\Delta u^{elastic} = 6\pi r_o^3 \frac{K_1^2}{K_1+\frac{4}{3}G_o}\left(\frac{r_1}{r_o}-1\right)^2\left[1+\frac{K_1}{K_1+\frac{4}{3}G_o}\left(\frac{r_1}{r_o}-1\right)\right]. \quad (20)$$

This equation contains the bulk modulus of a trace element (K_1) and the shear modulus of the matrix crystal (G_o). This corresponds to the fact that the strain inside of a spherical inclusion is homogeneous compression while the strain outside of an inclusion is shear strain (Eshelby, 1951, 1954, 1956). The effective elastic constant (the *EEC*, or the lattice strain parameter) corresponding to the Young's modulus in the Brice model would be $\frac{3K_1^2}{K_1+\frac{4}{3}G_0}$ that is related to the stiffness of the element as $EEC \approx 3K_1$ for $K_1 \gg G_o$, while $EEC \approx \frac{9}{4}\frac{K_1^2}{G_o}$ for $K_1 \ll G_o$. Therefore the influence of elasticity of trace elements is large when the elastic constant of the trace element is much different from that of the matrix minerals. These predictions of the model have important bearing on the interpretations of experimental observations (see Discussion).

Influence of excess charge: dielectric polarization energy and influence on strain

When a trace element goes to a site that is usually occupied by an ion with a different electrostatic charge, then there will be an excess charge, either positive or negative, relative to the perfect crystal at the site that the trace element occupies. The excess charge exerts electrostatic force to the surrounding ions. Due to this force, cations and anions will move to the opposite directions causing dielectric polarization. The

This is a preprint, the final version is subject to change, of the American Mineralogist (MSA)
Cite as Authors (Year) Title. American Mineralogist, in press.
(DOI will not work until issue is live.) DOI: http://dx.doi.org/10.2138/am-2016-5665

494 dielectric polarization energy caused by an excess electrostatic charge, $\Delta Z \cdot e$, is given by
495 (e.g., (Flynn, 1972)),
496
497 $$\Delta u^{dielectric} = \frac{(\Delta Z)^2 e^2}{2\tilde{r}\kappa} \quad (21)$$
498
499 where κ is the static dielectric constant and $\tilde{r}$ is the size of the defect. This energy
500 decreases with the size of the trace element, and hence the solubility of the element
501 increases with the size of the defect. However, the influence of the atomic size is weak
502 compared to that in the elastic strain energy (see equation (20) where $\left(\frac{r_i}{r_0} - 1\right)^2$ term
503 provides strong influence of the size of atoms (ions)). Its effect is to change the values of
504 partition coefficient by a similar amount for all the trace elements. Systematic differences
505 in the partition coefficients among different minerals (e.g., *Mg*-perovskite versus *Ca*-
506 perovskite) might be due to the difference in the static dielectric constant, κ, between
507 these minerals (see a later section).
508 The static dielectric constant is the sum of the contributions from electronic, ionic
509 and dipolar effects and the dielectric constant varies among different minerals (e.g.,
510 (Kittel, 1986)). In general, an ion with a large radius has a large electronic polarizability
511 that has an important contribution to the static dielectric constants. Ca^{2+} has substantially
512 higher electronic polarizability and hence *Ca*-bearing minerals tend to have a large
513 dielectric constant (e.g., (Shannon, 1993)).
514 Excess charge has another effect. A large part of the atomic displacement caused
515 by the excess charge is the anti-symmetric movement of cations and anions, i.e.,

This is a preprint, the final version is subject to change, of the American Mineralogist (MSA)
Cite as Authors (Year) Title. American Mineralogist, in press.
(DOI will not work until issue is live.) DOI: http://dx.doi.org/10.2138/am-2016-5665

dielectric polarization. However, near the vicinity of the excess charge, displacement of ions is large and can contribute to the elastic strain, $\varepsilon = \frac{\tilde{r}}{r_0} - 1$. Let us consider a case where Mg^{2+} at the M-site is replaced with Ar (i.e., Ar_M'' (Ar at the M-site with two negative effective charge)). In such a case, the effective negative charge (the negative charge relative to the perfect lattice) is present at the *M*-site that exerts a large force to the neighboring oxygen ions to cause their displacement away from the defect (Ar_M''). The similar effect was observed by (Spalt et al., 1973) for a vacancy in *KBr*. Consequently, one expects a larger elastic strain than expected from $\varepsilon = \frac{\tilde{r}}{r_0} - 1 = \frac{K_1}{K_1 + \frac{4}{3}G_o}\left(\frac{r_1}{r_0} - 1\right)$, leading to larger strain energy. I will come back to this issue when I discuss the partitioning of noble gases (see also **Appendix 2**).

Finally, excess charge has another effect: the effect caused by the charge balance. This is a *chemical* effect in the sense that in order to deal with the charge balance one must consider the interaction with other charged species. This issue will be discussed when I discuss the partitioning (dissolution) of noble gas elements and hydrogen (water).

Trace element dissolution in the melts

In the literature where the element partitioning between minerals and melts is discussed, it is often assumed that the sensitivity of element partitioning on the atomic (ionic) size of element is caused by the sensitivity of the solubility in minerals to atomic (or ionic) size of elements, and that the element dissolution in melts is associated with small excess energy and is insensitive to the size of elements (e.g., (Blundy and Wood, 2003)). This is the case for most trace elements.

Noble gases do not follow this: solubility is low and sensitive to the atomic size (Carroll and Stolper, 1993; Guillot and Sarda, 2006; Guillot and Sator, 2012; Heber et al., 2007; Shibata et al., 1998; Shibata et al., 1994). There is no clear evidence of the presence of a peak in the solubility coefficient when plotted against the size of noble gas atom. Therefore these observations suggest that noble gas atoms do not occupy well-defined sites. Carrol and Stolper (1993) explained this observation by a model in which noble gas atoms occupy the void space. Similarly, Guillot and his colleagues used a "hard sphere model" in which they assumed that noble gas atoms occupy the void space among the hard spheres (Guillot and Sarda, 2006; Guillot and Sator, 2012). The hard sphere model also explains the correlation between the composition and the solubility coefficient of noble gases: the noble gas solubility coefficient is higher in a melt with higher silica content (Shibata et al., 1998). Such a trend is often explained by the concept of *NBO* (non-bridging oxygen; (Mysen, 1983)), but this can also be explained by a hard sphere model because the degree of net-working increases with the increase of the silica content that leads to a higher void space (Guillot and Sarda, 2006; Guillot and Sator, 2012).

Given a marked dependence of noble gas solubility coefficient in the melt on their atomic size but a commonly made assumption of independence of other trace element dissolution on their ionic size, one may wonder why the dissolution behavior of these two types of elements in the melts is so different. In order to understand what controls the mechanisms of dissolution of elements in the melt, let us consider a hard sphere model of silicate melts (**Fig. 5**). Unlike minerals, complex liquids such as silicate melts can be considered as a mixture of clusters of atoms (hard spheres) that are randomly distributed leaving void space among them. Since these clusters are separated by the void space,

This is a preprint, the final version is subject to change, of the American Mineralogist (MSA)
Cite as Authors (Year) Title. American Mineralogist, in press.
(DOI will not work until issue is live.) DOI: http://dx.doi.org/10.2138/am-2016-5665

their direct mutual interaction is weak except that any cluster cannot move into the space occupied by other clusters ("excluded volume"). These clusters move nearly freely in the limited space (space unoccupied by other clusters) and hence the internal energy of a cluster does not change much with the type of liquid where it is located. Free motion of clusters in the limited space contributes to the configurational entropy, S_{config}, and $-T \cdot S_{config}$ makes the dominant contribution to the free energy of a complex liquid. The hard sphere model is one of these models and provides a systematic explanation of a large number of observations on the equation of state of melts (Jing and Karato, 2011).

Fig. 5a shows a case where a trace element (*i*) replaces a host element (*y*) in a molecular cluster in the liquid. This is a case where the element *i* has modest electric charge similar to the host ion *h*. The initial energy of the whole system is $u_{initial} = u_i^A + u_y^L$ ($u_{i.y}^{L,A}$: energy of a cluster in the liquid (*L*) or in the reservoir (*A*) containing the element *i* or *h*), and the final energy is $u_{final} = u_y^A + u_i^L$. Therefore $u_{final} - u_{initial} = \left(u_y^A - u_i^A\right) - \left(u_y^L - u_i^L\right)$. In a hard sphere model, clusters (hard spheres) do not interact each other energetically. Therefore the energy difference such as $u_y^{L,A} - u_i^{L,A}$ is the energy difference in the clusters and $u_y^L - u_i^L \approx u_y^A - u_i^A$, i.e., $u_{final} \approx u_{initial}$[7]. Since both elements *i* and *h* occupy the cluster, there is little change in the excluded volume and hence little change in the configurational entropy and $\mu_{final} \approx \mu_{initial}$. Consequently the solubility of these elements is high and nearly independent of their size.

[7] For a solid, $u_{i,h}^L \neq u_{i,h}^A$ because of the strong interaction among the clusters, and hence $u_{initial}^S \neq u_{final}^S$.

This is a preprint, the final version is subject to change, of the American Mineralogist (MSA)
Cite as Authors (Year) Title. American Mineralogist, in press.
(DOI will not work until issue is live.) DOI: http://dx.doi.org/10.2138/am-2016-5665

For a noble gas element that has neutral charge, there will be a large excess electrostatic energy if it replaces an ion in a cluster. Also the noble gas in the environment ("*A*") is not in the cluster, and a cation will not be dissolved in the noble gas. Consequently, the noble gas dissolution does not occur as an exchange of a noble gas atom and the cation in the liquid. Therefore the second mechanism (occupying the void space) will be preferred (**Fig. 5b**). In this case, the excess energy strongly depends on the size of the noble gas atom that determines the decrease in the void space (free volume).

DISCUSSION

Comparison with the previous strain energy models on element solubility in minerals

Elastic strain energy associated with the replacement of an ion in a mineral with a trace element is an important factor controlling the solubility of the trace element in a mineral (e.g., (Blundy and Wood, 2003)). In this section, I compare various strain energy models with the experimental observations. **Table 2** compares three models of the strain energy associated with the dissolution of an element in a mineral, and **Fig. 6** shows a graph of normalized solubility (~partition coefficient if the element solubility in the melt is independent of the size of the element) against $\frac{r_i}{r_o}$. All models show a peak in the solubility at the ionic radius corresponding to the radius of the site of the host crystal ($\frac{r_i}{r_o}$=1) (see equation (19)). The curvature of the curves is determined by the effective elastic constant $(EEC)_{obs}$ relevant to element substitution that can be defined as

$$\Delta u^{elastic} = 2\pi r_o^3 (EEC)_{obs} \left(\frac{r_i}{r_o} - 1\right)^2 \left[1 + \xi\left(\frac{r_i}{r_o} - 1\right)\right] \qquad (22)$$

This is a preprint, the final version is subject to change, of the American Mineralogist (MSA)
Cite as Authors (Year) Title. American Mineralogist, in press.
(DOI will not work until issue is live.) DOI: http://dx.doi.org/10.2138/am-2016-5665

where $\Delta u^{elastic}$ is the strain energy and $\xi = \frac{K_1}{K_1 + \frac{4}{3}G_o}$ for my model and $\xi = \frac{2}{3}$ for the Brice model[8]. Although all models show similar curves, the curvature, i.e., $(EEC)_{obs}$, has different expressions (see **Table 2**), and it is $(EEC)_{obs}$ that distinguishes different models. $(EEC)_{obs}$ was calculated by Blundy and Wood for various sites in various minerals. For each combination of the site and the mineral, experimental data on partitioning for various elements were used and from the shape of the curve of the Onuma diagram, they calculated $(EEC)_{obs}$ (see **Appendix 3**). In the following, I will use the values of $(EEC)_{obs}$ and compare them with the predictions from various models to evaluate the validity of the models.

The simplest model for $(EEC)_{calc}$ would be the Brice model where all the relevant elastic constants are those for the matrix. In this case,

$$(EEC)_{calc}^{Brice} = \frac{3K_oG_o}{K_o + G_o/3} \approx 1.5K_o = 0.225\frac{Z_o}{(r_o + r_{oxy})^3} \qquad (23)$$

where K_o (EEC) is in GPa, r in nm, and Z_o is the valence of the ion at the site (+2 for Mg^{2+}), r_o is the ionic radius of the site in the matrix that is replaced with the trace element, r_{oxy} is the ionic radius of oxygen (0.138 nm). The results are compared with $(EEC)_{obs}$ in **Fig. 7a**. The results show very poor fit indicating that the properties of a trace element other than its size play an important role in controlling the effective elastic

[8] The difference in ξ between these two models is small and does not affect the calculated values of $(EEC)_{obs}$ substantially.

This is a preprint, the final version is subject to change, of the American Mineralogist (MSA)
Cite as Authors (Year) Title. American Mineralogist, in press.
(DOI will not work until issue is live.) DOI: http://dx.doi.org/10.2138/am-2016-5665

623 constant, EEC. I evaluate the goodness of the model by a parameter χ^2 (reduced chi-
624 square or variance)[9] and χ^2=106 for this model.

625 Blundy and Wood (1994) noted a good correlation between $(EEC)_{obs}$ and Z_1
626 (charge of the trace element) in plagioclase and diopside ($(EEC)_{obs} \propto Z_1$). The EEC of
627 the M2 site of clinopyroxene systematically changes with the charge of the trace elements
628 in such a way that $(EEC)^{+1}_{M2} < (EEC)^{+2}_{M2} < (EEC)^{+3}_{M2}$ where $(EEC)^{+n}_{M2}$ is the effective elastic
629 modulus of the M2 site for trace elements with a charge +n (Blundy and Dalton, 2000).
630 Similarly, (Hill et al., 2011) found $(EEC)^{+3}_{M2} \square (EEC)^{+4}_{M1}$ for clinopyroxene although the
631 polyhedron bulk moduli for the M1 and M2 sites are similar (Levien and Prewitt, 1981).
632 The EEC for a given mineral and a given site varies as much as a factor of ~100 among
633 different trace elements. This challenges the theory because none of the previous theories
634 (Brice, 1975; Nagasawa, 1966) includes the properties of a trace element other than its
635 size.

636 To account for the strong influence of the electrostatic charge of the trace element
637 Z_1, Blundy and Wood proposed the following relationship,

638

639 $$(EEC)^{BW}_{calc} = 1.125 \cdot Z_1 / \left(r_o + r_{oxy}\right)^3 \qquad (24)$$

640

[9] χ^2 (reduced chi-square or normalized variance) is defined as $\chi^2 = \frac{1}{N}\sum_j \frac{\sum_i \left(y_j^i - x_j\right)^2}{\sum_i \left(y_j^i - \bar{y}_j\right)^2}$ where j specifies a combination of a mineral, the site and the charge of the trace element (j=1---N), and i specifies the individual data of EEC (i=1---M_j), y_j^i is the inferred value of EEC for a given i and j from the experimental data, x_j is the model prediction for j and $\bar{y}_j$ is the mean value of y_j^i. For the perfect model, χ^2=0.

This is a preprint, the final version is subject to change, of the American Mineralogist (MSA)
Cite as Authors (Year) Title. American Mineralogist, in press.
(DOI will not work until issue is live.) DOI: http://dx.doi.org/10.2138/am-2016-5665

641 and called this as "site-elasticity" ($(EEC)_{calc}^{BW}$ in GPa, r in nm) (Blundy and Wood, 1994).
642 A comparison of this model with $(EEC)_{obs}$ is shown in **Fig. 7b.** This model better fits
643 $(EEC)_{obs}$ (χ^2=40) but shows a systematic deviation from $(EEC)_{obs}$ for the large values
644 of *EEC*. Apart from the use of a dimensionally incorrect formula for an elastic constant[10],
645 the theoretical basis of combining the property of the trace element (Z_1) and the property
646 of the matrix (r_o) in the Blundy-Wood model is unclear.

647 In contrast to the previous models by (Nagasawa, 1966) and (Blundy and Wood,
648 1994), my model includes the influence of different elastic properties of the matrix and
649 the trace element based on the Eshelby theory of a point defect in an elastic material. This
650 model shows that the effective elastic constant (*EEC*) is $(ECC)_{calc}^{Karato} = \frac{3K_1^2}{K_1+\frac{4}{3}G_o}$.

651 According to this model, it is the bulk modulus of the trace element (K_1) and the
652 shear modulus of the matrix (G_o) that determine the *EEC*. The *EEC* is not the Young's
653 modulus of the material as incorrectly assumed by Brice (1975). For K_1, I use a
654 relationship $K_1 = 0.15 \cdot Z_1 / \left(r_1 + r_{oxy}\right)^4$ [11] corrected from (Hazen and Finger, 1979) and
655 calculated $(EEC)_{calc}^{Karato} = \frac{3K_1^2}{K_1+\frac{4}{3}G_o}$. In other words, I assume that K_1 is determined by the
656 bonding between the trace element and the surrounding oxygen ions. One problem with
657 this approach is that because $(EEC)_{obs}$ is calculated for each site (each r_o) for a range of

[10] The relation $(EEC)_{calc}^{BW} = 1.125 \cdot Z_1 / \left(r_o + r_{oxy}\right)^3$ is derived from Hazen and Finger (1979) model, $K = 0.75 \cdot Z / \left(r + r_{oxy}\right)^3$ (K in GPa, Z: charge of cation, r: radius of cation (nm)) but this equation is dimensionally incorrect (Karato, 2008). A dimensionally correct equation is $K = 0.15 \cdot Z / \left(r + r_{oxy}\right)^4$, but these two equations predict similar elastic constants.

[11] One could use a relation similar to Blundy-Wood's model, i.e., the use of r_o instead of r_1, $K_1 = 0.15 \cdot Z_1 / \left(r_o + r_{oxy}\right)^4$. The results are similar (not shown).

This is a preprint, the final version is subject to change, of the American Mineralogist (MSA)
Cite as Authors (Year) Title. American Mineralogist, in press.
(DOI will not work until issue is live.) DOI: http://dx.doi.org/10.2138/am-2016-5665

r_1 one must use some average of r_1. I used a simple arithmetic average. The calculated $(EEC)_{calc}^{Karato}$ are compared with $(EEC)_{obs}$ in **Fig. 7c** (for the details see **Appendix 3**). My model, $(EEC)_{calc}^{Karato}$, shows a better fit to $(EEC)_{obs}$ for large values of (EEC), and the variance is substantially reduced (χ^2=18 for this model). However, the use of the "bulk modulus" to represent the stiffness of a trace element is a gross simplification, and its limitation will become obvious when I analyze the solubility of noble gas elements.

Why do Ca-bearing minerals have high trace element solubility?

Solubility of trace elements is sensitive to minerals. Most trace elements have much higher solubility in clinopyroxene than olivine (e.g., (Witt-Eickschen and O'Neill, 2005)). Similarly, the trace element solubility in *Ca*-perovskite is higher than that in *Mg*-perovskite (e.g., (Corgne et al., 2004; Hirose et al., 2004)). Common to these two cases is that the solubility of trace elements is higher in a mineral that contains *Ca* than those that do not contain *Ca*.

Here I take an example of *Ca*-perovskite and *Mg*-perovskite (bridgmanite) for which a detailed study was conducted (Hirose et al., 2004). Although there is a large difference in $D_i^{mineral/melt}$ between *Ca*-perovskite and *Mg*-perovskite in the ionic size versus $D_i^{mineral/melt}$ plot (the Onuma diagram) implying that there is no large difference in $D_i^{mineral/melt,elastic}$ between them (**Fig. 1c**). Therefore I conclude that most of the difference between *Ca*-perovskite and *Mg*-perovskite (bridgmanite) is caused by the difference in $D_i^{mineral/melt,\,dielectric}$ term. The main physical property that controls $D_i^{mineral/melt,dielectric}$ is (static) dielectric constant, κ (equation (19)). The static dielectric constant of a mineral

This is a preprint, the final version is subject to change, of the American Mineralogist (MSA)
Cite as Authors (Year) Title. American Mineralogist, in press.
(DOI will not work until issue is live.) DOI: http://dx.doi.org/10.2138/am-2016-5665

680 depends on the polarizability of ions contained in a mineral (e.g., (Kittel, 1986)). Among
681 various cations in a typical mantle minerals, *Ca* has anomalously large polarizability due
682 to its large ionic size (Shannon, 1993). Consequently, a mineral that contains a large
683 amount of *Ca* has a large dielectric constant and hence leads to the high solubility of trace
684 elements.
685
686 *Partitioning of noble gases*
687 In previous sections, I pointed out that there are fundamental limitations of the
688 previous models of element partitioning in incorporating the elasticity of trace elements.
689 This problem becomes serious when one deals with noble gas elements whose elastic
690 constants are much lower than those of the host minerals (e.g., ~2-4 GPa (Devlal and
691 Gupta, 2007; Jephcoat, 1998) as compared to ~120 GPa for olivine).
692 Brooker et al. (2003) suggested that the observed trend for *partitioning* of noble
693 gases showing the weak dependence on noble gas atomic size (**Fig. 1e**) can be attributed
694 to weak effective elastic constants (a 'zero charge' model). However, such an explanation
695 is misleading for two reasons. First, the weak dependence of *partition coefficient* on the
696 atomic size of noble gas elements observed in the diagram such as **Fig. 1e** does not mean
697 that the *solubility* of noble gas elements in olivine and diopside depends weakly on the
698 atomic size of noble gas elements. The partition coefficient shown in **Fig. 1e** is the ratio
699 of the solubility of noble gas in a mineral to that in a melt (see equation (12),
700 $D_{noble\ gas}^{mineral/melt} = \frac{C_{noble\ gas}^{mineral}}{C_{noble\ gas}^{melt}}$; $C_{noble\ gas}^{mineral,melt}$: concentration of noble gas in mineral (melt)). The
701 experimental observations shown in **Fig. 1e** indicate that $D_{noble\ gas}^{mineral/melt}$ is weakly dependent
702 on the size of the noble gas atom. But $C_{noble\ gas}^{melt}$ is strongly dependent on the size of the

This is a preprint, the final version is subject to change, of the American Mineralogist (MSA)
Cite as Authors (Year) Title. American Mineralogist, in press.
(DOI will not work until issue is live.) DOI: http://dx.doi.org/10.2138/am-2016-5665

noble gas atom (Carroll and Stolper, 1993; Heber et al., 2007; Shibata et al., 1998; Shibata et al., 1994) (**Fig. 1f**). Therefore, one must conclude that $C_{noble\ gas}^{mineral}$ is strongly dependent on the size of noble gas atoms.

To illustrate this point, I calculated $C_{noble\ gas}^{mineral}$ for olivine and diopside from the results shown in **Fig.1e** ($D_{noble\ gas}^{mineral/melt}$) and **Fig. 1g** ($C_{noble\ gas}^{melt}$). **Fig. 8** shows a plot of partition coefficients of noble gases between olivine (or diopside) and the melt multiplied by the solubility of noble gases in the melts, $D_{noble\ gas}^{mineral/melt} \cdot C_{noble\ gas}^{melt}$. Essentially this is a plot of the solubility (coefficient) of noble gases, $C_{noble\ gas}^{mineral}\left(= D_{noble\ gas}^{mineral/melt} \cdot C_{noble\ gas}^{melt}\right)$, in olivine and diopside as a function of the size of noble gas atoms. This plot shows that the solubility of noble gases in olivine and diopside decreases substantially with the size of the noble gas atom. A similar trend was reported for the noble gas solubility in bridgmanite (Shcheka and Keppler, 2012) (**Fig. 1f**). I conclude that the solubility of noble gases in olivine, diopside and bridgmanite decreases strongly with the atomic size of noble gas, and therefore these results are *inconsistent* with the 'zero-charge' model by (Brooker et al., 2003).

Second, the model by (Brice, 1975) does not include the stiffness of the trace element and the concept of "site-elasticity" in which one invokes the stiffness of the trace element does not have a sound physical basis as discussed before. The elastic constant in the Brice model is the elastic constant of the matrix. So even though a noble gas element has 'zero charge', one should not make the effective elastic constant = 0 if one were to use the Brice model. However, my model in its simplest form also fails to explain this observation. If one uses experimentally determined bulk moduli of noble gas elements

(Devlal and Gupta, 2007; Jephcoat, 1998) with my theory (equation (20)), one would predict that the effective elastic constant will be $\frac{3K_1^2}{K_1+\frac{4}{3}G_o}$~0.3 GPa. This is too low to explain the observations. One might try to explain this by dielectric polarization model as Brooker et al. (2003) proposed. However, the dielectric polarization model predicts an opposite trend (high solubility for a large size).

How can we interpret such a trend, i.e., the substantial reduction of the solubility of noble gas elements with their atomic size? Let us use a strain energy model and interpret the inferred "bulk modulus" of the noble gas based on a physical model of point defects in ionic solids. Because the data are limited, I assume r_o and using the solubility versus atomic size (r_1) relation, I will estimate the effective elastic constant. The observed trend (**Fig. 8**) suggests that the size of the site (r_o) where a noble gas atom is located in olivine and diopside must be smaller than 0.16 nm (atomic size of *Ar*). Assuming that r_o =0.072 nm in olivine, I get ~12 GPa (for clinopyroxene, assuming r_0 =0.1 nm, I get ~20 GPa). Similarly, Shcheka and Keppler (2012) estimated the effective elastic constant in bridgmanite is ~35 GPa assuming that noble gas elements go to the oxygen site (r_0 =0.14 nm). These effective elastic constants are substantially larger than those estimated from the bulk moduli of the noble gases and the shear modulus of the matrix using the definition of the effective elastic modulus, $\frac{3K_1^2}{K_1+\frac{4}{3}G_o}$ (~0.2-0.3 GPa).

The *ECCs* of the noble gas elements inferred from the experimental observations of element partitioning are much higher than those calculated from the experimentally determined elastic moduli of relevant elements. There is a possible physical explanation for the inferred high *ECC*. When one inserts an atom into a crystalline site, then both

crystal and the atom deform to define the equilibrium size of the site (equation (19)). If one uses the bulk modulus of the sphere, K_1 (2-4 GPa), then the lattice strain will be $\varepsilon = \frac{\tilde{r}}{r_0} - 1 = \frac{K_1}{K_1 + \frac{4}{3}G_o}\left(\frac{r_1}{r_o} - 1\right)$ and for a typical bulk moduli of noble gas element, the strain will be on the order of 1-2 % of $\left(\frac{r_1}{r_o} - 1\right)$. For $\left(\frac{r_1}{r_o} - 1\right)$~20 %, the lattice strain would be ~0.3 %. Inferred high effective elastic strain implies that the atomic displacement near the "defect" site (where a trace element replaces a host ion) is larger than expect from such a model. This can be explained if one considers the force balance at the site where a noble gas atom is inserted from a more atomistic point of view. When a neutral atom (e.g., a noble gas atom) replaces a cation (e.g., Mg^{2+}), then there will be excess 2- charge at the site that will exert a repulsive force to the neighboring oxygen ions. As a consequence, neighboring oxygen ions move outward (see (Spalt et al., 1973) for a case of a vacancy in *KBr*). Consequently, the lattice strain caused by the replacement of a cation (e.g., Mg^{2+}) with a noble gas will be larger than what one expects from the simple elastic model. The inferred large effective elastic constant for a noble gas could be due to this effect. In other words, the noble gas solubility in minerals such as olivine is likely much lower than expected from the low bulk moduli of the noble gases. I note that using a theoretical approach Du et al. (2008) showed relatively large effective elastic moduli for the dissolution of noble gases in minerals (Du et al., 2008).

How can one explain the large difference in the magnitude of noble gas solubility between bridgmanite and other minerals (olivine and diopside)? To address this issue, let us consider the processes of noble gas dissolution in more detail. **Fig. 9** shows two possible mechanisms of noble gas dissolution in minerals. In **Fig. 9a**, a noble gas atom,

This is a preprint, the final version is subject to change, of the American Mineralogist (MSA)
Cite as Authors (Year) Title. American Mineralogist, in press.
(DOI will not work until issue is live.) DOI: http://dx.doi.org/10.2138/am-2016-5665

769 Π, occupies the M-site vacancy and in **Fig. 9b**, it occupies the O-site vacancy. In both
770 cases, the concentration of noble gas atoms in the mineral is related to the concentration
771 of vacancies as
772
773 $$\left[\Pi_{\Phi}^{\Psi}(P,T,f_{O2},a_{SiO2})\right] \propto \left[V_{\Phi}^{\Psi}(P,T,f_{O2},a_{SiO2})\right] \cdot f_{\Pi}(P,T) \cdot K_{\Pi}(P,T,f_{O2},a_{SiO2}) \quad (25)$$
774
775 where Π_{Φ}^{Ψ} is a noble gas atom occupying the Φ-site with an effective charge of Ψ (e.g.,
776 Ar_M'' (*Ar* at the M-site with effective two negative charge)), V_{Φ}^{Ψ} is a vacancy at the Φ-site
777 with an effective charge of Ψ, f_{Π} is the fugacity of the noble gas Π, and K_{Π} is the
778 relevant equilibrium constant[12].
779 The strain energy consideration discussed above was on K_{Π}. The equilibrium
780 constant, $K_{\Pi}(P,T,f_{O2},a_{SiO2})$, depends on the excess energy of a mineral when vacancy is
781 occupied by a noble gas. However, the difference in this term between olivine, diopside
782 and bridgmanite is not consistent with the difference in the noble gas solubility among
783 these minerals. Therefore I conclude that it is the difference in vacancy concentration,
784 $\left[V_{\Phi}^{\Psi}\right]$, that is responsible for the difference in the solubility of noble gases in different
785 minerals.
786 The concentration of vacancy depends strongly on minerals. In case of olivine and
787 diopside, the relevant vacancy is V_M'' whose concentration is ~10^{-5}-10^{-4} under typical
788 upper mantle conditions (Nakamura and Schmalzried, 1983), whereas in bridgmanite the

[12] To clarify the microscopic aspect, I used a point-defect notation, i.e., Kröger-Vink notation, $\left[\Pi_{\Phi}^{\Psi}\right]$ rather than $C_{noble\,gas}^{mineral}$.

This is a preprint, the final version is subject to change, of the American Mineralogist (MSA)
Cite as Authors (Year) Title. American Mineralogist, in press.
(DOI will not work until issue is live.) DOI: http://dx.doi.org/10.2138/am-2016-5665

dominant vacancy is $V_O^{\square}$ whose concentration is much higher although it depends on the concentration of impurities such as Al^{3+} (e.g., (Brodhlot, 2000; Lauterbach et al., 2000; Navrotsky, 1999)). This provides an explanation for the higher solubility of noble gases in bridgmanite compared to olivine and diopside (e.g., (Brooker et al., 2003; Shcheka and Keppler, 2012)). However, this model also implies that the solubility is highly pressure dependent, $\left[\Pi_{\Phi}^{\Psi}\right] \propto exp\left(-\frac{PV^*}{RT}\right)$, where V^* is the volume expansion associated with vacancy formation.

SOME APPLICATIONS

Water content in the mantle from mantle materials

Among the various elements, volatile elements such as *H* play important roles in a number of geological processes and therefore estimating the water content in the mantle is an important topic (e.g., (Karato, 2011; Peslier et al., 2010)). However, because of very high mobility of *H* in olivine (and other minerals or melts; (Kohlstedt and Mackwell, 1998)), it is challenging to infer the distribution of *H* in the mantle. Evidence of hydrogen-loss from olivine is frequently reported (e.g., (Demouchy et al., 2006; Peslier and Luhr, 2006)). Two approaches have been conducted to overcome this difficulty.

One is to measure the water content of other minerals such as orthopyroxene where hydrogen diffusion is more sluggish (inferred from the lack of diffusion profile in opx; (Warren and Hauri, 2014)). In such a case, one might consider that the hydrogen content in orthopyroxene is more "reliable" and could take it as a more faithful indicator of *H* in the mantle. However, different water content between olivine and orthopyroxene may also reflect the equilibrium partitioning that depends on the thermodynamic

This is a preprint, the final version is subject to change, of the American Mineralogist (MSA)
Cite as Authors (Year) Title. American Mineralogist, in press.
(DOI will not work until issue is live.) DOI: http://dx.doi.org/10.2138/am-2016-5665

812 conditions. A careful analysis must be made including the influence of the dependence of
813 hydrogen partition coefficient on the thermochemical conditions. The water partitioning
814 between olivine and orthopyroxene,
815
816 $$\frac{[H]_{oli}}{[H]_{opx}} \propto \frac{f_{H2O}^{\alpha_{oli}}}{f_{H2O}^{\alpha_{opx}}} \frac{exp\left(-\frac{E_{oli}^{H}+PV_{oli}^{H}}{RT}\right)}{exp\left(-\frac{E_{opx}^{H}+PV_{opx}^{H}}{RT}\right)} \quad (26)$$

817
818 where $\alpha_{oli,opx}$ is the fugacity coefficient, $E_{oli.opx}^{H}$ and $V_{oli.opx}^{H}$ are energy and volume change
819 associated with hydrogen dissolution in olivine and orthopyroxene respectively. Because
820 all of these parameters are different between olivine and orthopyroxene (Kohlstedt et al.,
821 1996; Mierdel et al., 2007), the water partition coefficient, $\frac{[H]_{oli}}{[H]_{opx}}$, changes with the
822 thermodynamic conditions by more than a factor of 10 (Dai and Karato, 2009).
823 Particularly important is the fact that in most cases, $\frac{[H]_{oli}}{[H]_{opx}} \propto f_{H2O}^{1/2}$, and consequently, the
824 partition coefficient of water (hydrogen) between olivine an opx is depends on water
825 fugacity. Consequently, under the environment where water fugacity is low (e.g., the
826 lithosphere), the partition coefficient is low and much of water (hydrogen) in the
827 lithosphere goes to orthopyroxene. In many literatures, the observed low $\frac{[H]_{oli}}{[H]_{opx}}$ in the
828 lithosphere is interpreted to be a results of hydrogen loss from olivine, and the water
829 content in orthopyroxene is used to estimate the water content in the lithosphere
830 assuming the partition coefficient determined at high water fugacity (e.g., (Warren and
831 Hauri, 2014)). This method could lead to an over-estimate of the water content in the

This is a preprint, the final version is subject to change, of the American Mineralogist (MSA)
Cite as Authors (Year) Title. American Mineralogist, in press.
(DOI will not work until issue is live.) DOI: http://dx.doi.org/10.2138/am-2016-5665

lithosphere. Also, I note that (Hauri et al., 2006; Tenner et al., 2009) and (Mierdel et al., 2007) reported quite different depth dependence of *H* solubility and partitioning.

Ce/H ratio ($\frac{[Ce]}{[H]}$) of basaltic magma is often used to infer the hydrogen content in the source region (e.g., (Dixon et al., 2002)). Again there are two concepts behind this approach. First, both *Ce* and *H* are "incompatible elements" and go mostly to the melt upon partial melting. The degree to which pre-existing *Ce* and *H* in the rock goes to melt depends on the partition coefficients (if everything occurs as equilibrium process). The assumption behind this is that this ratio is nearly constant and hence by knowing the concentration of *Ce*, one could get some idea about the *H* content in the source region. Also the diffusion of *Ce* is much slower than that of *H* (e.g., (Chakraborty, 2010)) so *Ce* will faithfully reflect the *Ce* content of the source region while *H* might have escaped. Another also important assumption behind this exercise is that the partition coefficient of *Ce* and *H* between minerals and melts does not change with physical/chemical conditions.

Since *H* and *Ce* have different electrostatic charges (normally H^+ and Ce^{3+}), the dissolution mechanisms of *H* and *Ce* are likely different (**Fig. 10**). The dissolution mechanisms illustrated in **Fig. 10** lead to the following relationship,

$$\frac{[Ce]}{[H]} \propto \frac{a_{Ce_2O_3}^{1/2}}{f_{H_2O}} f_{O_2}^{-1/12} exp\left[-\frac{P\left(\frac{3\upsilon_{Mg}-2\upsilon_{Ce}}{2}-\upsilon_{MgO}\right)}{RT}\right] \quad (27)$$

where $a_{Ce_2O_3}$ is the activity of Ce_2O_3, f_{O2} is oxygen fugacity (where I assumed a relation $[V_M''] \propto f_{O2}^{1/6}$), υ_{MgO} is the molar volume of MgO, υ_{Mg} is the molar volume of Mg and υ_{Ce}

This is a preprint, the final version is subject to change, of the American Mineralogist (MSA)
Cite as Authors (Year) Title. American Mineralogist, in press.
(DOI will not work until issue is live.) DOI: http://dx.doi.org/10.2138/am-2016-5665

854 is the molar volume of *Ce*. Among various terms in the right hand side of this equation,
855 $a_{Ce_2O_3}$ and f_{H2O} correspond to the composition of the material, whereas other terms
856 (f_{O2}, $exp\left[\frac{P\left(\upsilon_{MgO}-\frac{3\upsilon_{Mg}-2\upsilon_{Ce}}{2}\right)}{RT}\right]$) depend on the physical and chemical conditions. In particular,
857 since $\left(\upsilon_{MgO}-\frac{3\upsilon_{Mg}-2\upsilon_{Ce}}{2}\right)>0$, the ratio $\frac{[Ce]}{[H]}$ increases with pressure. The depth (therefore pressure
858 and temperature) at which partial melting occurs is different among different types of
859 volcanism (e.g., mid-ocean ridge volcanism versus ocean island volcanism). Therefore
860 the ratio $\frac{[Ce]}{[H]}$ is likely different among the rocks from different regions. Also, the
861 diffusion coefficient of *Ce* is much lower than that of *H* (Van Orman et al., 2001).
862 Therefore it is possible that *Ce* concentration is not in chemical equilibrium.
863
864 *Are noble gases compatible or incompatible elements?*
865 Noble gases are often assumed to behave like incompatible elements (e.g.,
866 (Allègre et al., 1996; Marty, 2012)). However, this notion is not entirely secure because
867 either a noble gas element behaves like a compatible or incompatible element depends on
868 the solubility ratio of that element between minerals and melts, and the solubility of noble
869 gases in both minerals and melts depends strongly on pressure and temperature and
870 minerals. Consequently, it is possible that the behavior of the noble gas elements, either
871 compatible or incompatible, depends on the conditions at which melts and minerals co-
872 exist.
873 There have been some challenges to the common belief of incompatible element
874 behavior of noble gases such as *Ar*. For instance, Watson et al. (2007) published the
875 results suggesting that *Ar* is a compatible element in the upper mantle although most of

This is a preprint, the final version is subject to change, of the American Mineralogist (MSA)
Cite as Authors (Year) Title. American Mineralogist, in press.
(DOI will not work until issue is live.) DOI: http://dx.doi.org/10.2138/am-2016-5665

876 previous studies show that all the noble gas elements behave like incompatible elements
877 in the upper mantle (e.g., (Broadhurst et al., 1992; Brooker et al., 2003)). Similarly,
878 Shcheka and Keppler (2012) published the experimental results showing high solubility
879 of *Ar* in bridgmanite suggesting that *Ar* might behave like a compatible element in the
880 lower mantle, although the solubility of other heavier noble gases is lower.

881 However, the validity of the conclusions by (Watson et al., 2007) is questionable.
882 The solubility of *Ar* reported by (Watson et al., 2007) are substantially higher than any
883 other results including those by (Hiyagon and Ozima, 1986) who reported relatively high
884 partition coefficient (high solubility) that is considered to be caused by inclusions (e.g.,
885 (Broadhurst et al., 1992)). If we focus on the results where the influence of inclusions
886 was minimized (e.g., (Broadhurst et al., 1992)), the difference is even larger. The reason
887 for the reported high solubility is unknown but one possibility is that this is due to the
888 anomalous properties near the surface[13] (see also (Pinilla et al., 2012)). In contrast,
889 Shcheka and Keppler (2012) measured the bulk composition and showed that
890 bridgmanite has much higher solubility of *Ar* than ringwoodite, and olivine. They also
891 found a systematic trend in the solubility of various noble gas elements (**Fig. 1e**).

892 In order to address the question of either a given noble gas behaves like an
893 incompatible element or compatible element during melting or crystallization, it is
894 necessary to compare the solubility of each noble gas element in minerals and melts.
895 I assume the results by (Broadhurst et al., 1992) on the solubility of *Ne, Ar, Kr* and *Xe* in
896 olivine and those in bridgmanite by (Shcheka and Keppler, 2012) in comparison with the

[13] Watson et al. (2007) used near surface ~ 60 nm layers. They checked the crystallinity of studied regions by electron-back scattered pattern (EBSD) but this does not prove that these regions are defect-free.

This is a preprint, the final version is subject to change, of the American Mineralogist (MSA)
Cite as Authors (Year) Title. American Mineralogist, in press.
(DOI will not work until issue is live.) DOI: http://dx.doi.org/10.2138/am-2016-5665

897 experimental results on the solubility in the melts by (Heber et al., 2007). Either a noble
898 gas element behaves like a compatible or incompatible element depends on the partition
899 coefficient, $D = \frac{C^{mineral}}{C^{melt}}$. A few assumptions are made in this analysis. First, the solubility
900 results by (Broadhurst et al., 1992) are reported as $[\Pi]/f_{\Pi}$ (solubility divided by the
901 fugacity of relevant element). However, the solubility depends on fugacity as well as the
902 free energy difference between a mineral with impurity and pure mineral as
903 $[\Pi] \propto f_{\Pi} exp\left(-\frac{E^*+PV^*}{RT}\right)$ (see equation (13)). Therefore one needs to make a correction for
904 the $exp\left(-\frac{E^*+PV^*}{RT}\right)$ term. The reported values by (Shcheka and Keppler, 2012) are directly
905 $[\Pi]$ but the results are at P=25 GPa (T=1873-2073 K). Therefore in order to discuss the
906 partitioning in the whole lower mantle (P=24 to 135 GPa, T=2000-4000 K), one needs a
907 large extrapolation in the $exp\left(-\frac{E^*+PV^*}{RT}\right)$ term. Given a vacancy model (**Fig. 9**), V^* is
908 essentially the volume change associated with vacancy formation that is approximately
909 the volume of ion that is replaced with a noble gas[14], and E^* can be estimated from the
910 experimental results (**Fig. 1e**) using the strain energy model.
911 *Ar* solubility in the melts at ~25 GPa calculated from the data at ~10 GPa
912 (Chamorro-Perez et al., 1998; Schmidt and Keppler, 2002) is ~0.1 wt % in olivine melt,
913 and 0.5-0.8 wt % tholeiite melt. The *Ar* solubility in bridgmanite at ~25 GPa is ~0.5-1 wt
914 % (Shcheka and Keppler, 2012). This means that the frequently made assumption that *Ar*
915 is incompatible element (e.g., (Allègre et al., 1996; Marty, 2012)) is not valid at least in
916 the shallow lower mantle, and bridgmanite will work as a reservoir for *Ar* in the shallow
917 lower mantle. For other noble gas elements, data are limited, but *Xe* has higher solubility

[14] This is based on the fact that oxygen is highly non-ideal gas at pressures higher than ~1 GPa.

This is a preprint, the final version is subject to change, of the American Mineralogist (MSA)
Cite as Authors (Year) Title. American Mineralogist, in press.
(DOI will not work until issue is live.) DOI: http://dx.doi.org/10.2138/am-2016-5665

in the melt than in bridgmanite, i.e., *Xe* is incompatible element at the shallow lower mantle.

However, the behavior of noble gas elements under higher pressures is not constrained. A theoretical model for the solubility in the melt suggests a modest decrease in solubility at higher pressures (Guillot and Sarda, 2006), while a vacancy model (see **Fig. 9**) would predict a stronger effect (with V^*=5 cc/mol, increase in pressure by 50 GPa will reduce the solubility by a factor of ~10^5) whereas the pressure effect on the solubility in melt is much less according to (Guillot and Sarda, 2006). Consequently, it is expected that the compatible element behavior of *Ar* is limited to the shallow lower mantle conditions. This hypothesis needs to be tested by experiments.

SUMMARY AND CONCLUDING REMARKS

Extensive experimental studies on trace element partitioning have revealed various trends including the importance of the difference in the size of the trace element and the size of the ion that the trace element replaces. The nature of element partitioning between two materials depends on how those materials accommodate "impurities". Physics and chemistry of point defects is highly relevant to understand the dissolution of trace elements. A continuum model of point defects (e.g., (Eshelby, 1951, 1954, 1956; Flynn, 1972)) and the basics of point defect chemistry (e.g., (Kröger and Vink, 1956)) can be used to explain a majority of observations. However, I also note that some atomistic details need to be incorporated in case of charged defects (e.g., (Mott and Littleton, 1938)) to explain the inferred magnitude of the strain field. In melts, impurities are accommodated by a more flexible structure. A hard sphere model (Barrat and Hansen,

2003; Guillot and Sarda, 2006; Guillot and Sator, 2012; Jing and Karato, 2011) provides a good framework to explain various behavior of trace element solubility in the melts.

One important general conclusion is that the solubility and/or the partition coefficient of any elements depends on minerals and melts as well as pressure, temperature and other chemical parameters (such as oxygen fugacity and water fugacity). Consequently, partition coefficients likely change with physical and chemical conditions. Results obtained under limited conditions should not be applied to other conditions without appropriate corrections. Experimental studies under a broad range of conditions are important to understand the behavior of elements in Earth and planetary interiors.

ACKNOWLEDMENT

I thank Keith Putirka for inviting me to write this review for the centennial volume of American Mineralogist. I thank Paul Asimow, Jon Blundy, Bernard Marty, Eiji Ohtani, Jim Van Orman, Zhengrong Wang and Bernie Wood for discussions. Jon Blundy kindly provided me with a digital data set corresponding to Fig. 5 of (Blundy and Wood, 2003) that was used to prepare Fig. 7 in the present paper.

I thank Jon Blundy and Cin-Ty Lee for constructive reviews.

This work is partially supported by NSF and NASA.

This is a preprint, the final version is subject to change, of the American Mineralogist (MSA)
Cite as Authors (Year) Title. American Mineralogist, in press.
(DOI will not work until issue is live.) DOI: http://dx.doi.org/10.2138/am-2016-5665

960 **Figure Captions**

961 **Fig. 1** Examples of some observations on element partitioning (solubility)

962 **a.** Element partition coefficient between diopside and silicate melt (Blundy and
963 Wood, 2003) (P=3 GPa, T=1930 K)

964 **b.** Trace element partition coefficients between (i) Mg-perovskite and silicate melt
965 and (ii) Ca-perovskite and silicate melt (Hirose et al., 2004) (P=25-27 GPa, T=2670-
966 2800K)

967 **c.** Trace element partition coefficients between (i) Mg-perovskite and silicate melt
968 and (ii) Ca-perovskite and silicate melt plotted as a function of the size of trace element,
969 i.e., the Onuma diagram (Hirose et al., 2004) (P=25-27 GPa, T=2670-2800K)

970 **d.** The partition coefficient of hydrogen between olivine and orthopyroxene (Dai and
971 Karato, 2009)

972 **e.** The partition coefficient of noble gas between olivine and silicate melt (Brooker
973 et al., 2003; Heber et al., 2007) (P=0.1 GPa, T=1530 K)

974 **f.** The solubility of noble gas elements in bridgmanite at P=25 GPa, T=1873-2073 K
975 (Shcheka and Keppler, 2012)

976 **g.** The solubility coefficient of noble gas in silicate melts at P=0.1 GPa and T~1530
977 K (Heber et al., 2007)

978

979 **Fig. 2** Two ways of examining the element partitioning between a solid (a mineral) and
980 a liquid (melt)

981 (a) Direct exchange of a trace element (*i*) and the host ion (*h*) (a model used by
982 (Blundy and Wood, 1994))

This is a preprint, the final version is subject to change, of the American Mineralogist (MSA)
Cite as Authors (Year) Title. American Mineralogist, in press.
(DOI will not work until issue is live.) DOI: http://dx.doi.org/10.2138/am-2016-5665

(b) The same process can be envisioned as the dissolution of a trace element (*i*) in a solid (a mineral) and a liquid (melt) (a model used in this paper).

Fig.3 A diagram showing the process of replacement of an ion with the radius r_o with a trace element with the radius r_1

The final size of the site ($\tilde{r}$) is between initial size (r_o) and the size of the trace element (r_1) and is determined by the size difference and the elastic properties of the matrix and the trace element.

Fig. 4 A plot of $\frac{\frac{\tilde{r}}{r_o}-1}{\frac{r_1}{r_o}-1}=\frac{K_1}{K_1+\frac{4}{3}G_o}=\frac{K_1/G_0}{1+\frac{4}{3}(K_1/G_0)}$ against K_1/G_0 ($\tilde{r}$: the size of the site after a trace element occupies replaces the pre-existing cation, r_o: the size of the site before a trace element goes to the site (size of the cation), r_1: the size of the trace element, K_1: the bulk modulus of the trace element, G_o: shear modulus of the matrix)

If the trace element is soft ($K_1/G_0 \to 0$; e.g., a noble gas element), then $\tilde{r} \approx r_o$, whereas if the trace element is stiff ($K_1/G_0 \to \infty$), $\tilde{r} \approx r_1$. The assumption by (Brice, 1975) of $\tilde{r} \approx r_1$ would be valid only for an infinitely stiff trace element, but not for weak elements such as the noble gas elements.

Fig. 5 A schematic diagram showing the processes of trace element dissolution in a liquid (*L*: liquid, *A*: reservoir)

(a) A case where a trace element (*i*) replaces a host ion (*h*) in the liquid

This is a preprint, the final version is subject to change, of the American Mineralogist (MSA)
Cite as Authors (Year) Title. American Mineralogist, in press.
(DOI will not work until issue is live.) DOI: http://dx.doi.org/10.2138/am-2016-5665

This is a case when the trace element is an ion occupying a cluster in the liquid and in the reservoir. The green hexagons in these figures show the clusters each of which contains a cation and oxygen ions.

(b) A case where a trace element (*i*) occupies the void space

This would be a preferred case when the trace element is neutral (e.g., noble gas). Dissolution of a trace element (noble gas atom) occurs as an addition to the liquid not as an exchange between the liquid (*L*) and the reservoir (*A*).

Fig. 6 Plots of normalized trace element solubility ($C_i^{mineral}$) corresponding to the elastic strain energy model against the size of the trace element corresponding to three models summarized in **Table 2** (r_1: size of the trace element, r_0: size of the site to which a trace element goes)

K_1=100 GPa ($=K_o$), G_0 =80 GPa, r_0= 0.1 nm, T=1600 K

The comparison is made after normalizing that the strain energy at r1/ro=1 is common. Such a diagram can be directly translated to a diagram for the partition coefficient ($D_i^{mineral/melt} = C_i^{mineral} / C_i^{melt}$) only when the concentration of trace element (C_i^{melt}) is independent of element.

Fig. 7 Plots showing the correlation of experimentally determined effective elastic constant $(EEC)_{obs}$ with the effective elastic constant from various models $(EEC)_{calc}$

amp: amphibole, cpx: clinopyroxene, gt: garnet, oli: olivine, opx: orthopyroxene, pla: plagioclase, woll: wollastonite (data from (Blundy and Wood, 2003)), unit of *EEC* is GPa

This is a preprint, the final version is subject to change, of the American Mineralogist (MSA)
Cite as Authors (Year) Title. American Mineralogist, in press.
(DOI will not work until issue is live.) DOI: http://dx.doi.org/10.2138/am-2016-5665

1026 (a) A comparison with the Brice model $(EEC)_{calc}^{Brice} = 0.225 \cdot Z_o / \left(r_o + r_{oxy}\right)^4$ (Z_o: electric
1027 charge of ion at the site where a trace element is dissolved, r_o: ionic radius of the host
1028 ion, r_{oxy}: ionic radius of oxygen ion)

1029 A thick line corresponds to $(EEC)_{obs} = (EEC)_{calc}^{Brice}$ ($\chi^2 = 106$).

1030 (b) A comparison with the Blundy and Wood model $(EEC)_{calc}^{BW} = 1.12 \cdot Z_1 / \left(r_o + r_{oxy}\right)^3$
1031 (Z_1: electric charge of the trace element)

1032 A thick line corresponds to $(EEC)_{obs} = (EEC)_{calc}^{BW}$ ($\chi^2 = 40$).

1033 (c) A comparison with the present model $(EEC)_{calc}^{Karato} = \frac{3K_1^2}{K_1 + \frac{4G_o}{3}}$

1034 K_1 is the bulk modulus of a cation-oxygen polyhedron ($= 0.15 \cdot Z_1 / \left(r_i + r_{oxy}\right)^4$, r_i: ionic
1035 radius of a trace element *i*). Since several different ions are used to determine $(EEC)_{obs}$, I
1036 used an average value, $\langle K_1 \rangle$ (average on various *i*). A thick line corresponds to
1037 $(EEC)_{obs} = (EEC)_{calc}^{Karato}$ ($\chi^2 = 18$).

1038

1039 **Fig. 8** Solubility of noble gases in olivine and diopside ($C_{noble\ gas}^{mineral}$) calculated from the
1040 partitioning coefficient $D_{noble\ gas}^{mineral/melt}$ and noble gas solubility in the melt $C_{noble\ gas}^{melt}$ using a
1041 formula $C_{noble\ gas}^{mineral} = D_{noble\ gas}^{mineral/melt} \cdot C_{noble\ gas}^{melt}$

1042 The data shown in **Fig. 1d** and **Fig. 1f** are used**.** The results correspond to P=0.1
1043 MPa and T~1550 K. Solubility of noble gases in the melt increases with pressure linearly
1044 to ~10 GPa (Guillot and Sarda, 2006). Solubility of noble gases in minerals also likely

This is a preprint, the final version is subject to change, of the American Mineralogist (MSA)
Cite as Authors (Year) Title. American Mineralogist, in press.
(DOI will not work until issue is live.) DOI: http://dx.doi.org/10.2138/am-2016-5665

increases with pressure linearly in the low-pressure regime (<0.1 GPa) (Henry's law), but the pressure dependence at high pressures was not studied.

Fig. 9 Dissolution of a noble gas element, Π, in a mineral via a vacancy mechanism

A noble gas atom (Π) goes into a vacant Φ-site to form a point defect $\Pi_{\Phi}^{\Psi'}$ (Π occupying the Φ-site with an effective charge of Ψ). A vacancy at the M-site (V_M'') is preferred in olivine and diopside while a vacancy at the O-site ($V_O^{\square}$) is preferred in bridgmanite. The charge compensating defects are $Fe_M^{\square}$ (ferric Fe at the M-site) in olivine and diopside, and e' (free electron) in bridgmanite.

Fig. 10 Models of dissolution of (a) *H* (hydrogen) and (b) *Ce* in olivine

(a) H_2O reacts with olivine to form *H*-bearing olivine (as $(2H)_M^{\times} + MgO_{surface}$)

This model predicts $[H] \propto f_{H2O}(P,T) \cdot exp\left(-\frac{P \cdot v_{MgO}}{RT}\right)$.

(b) Ce_2O_3 reacts with olivine to form *Ce*-bearing olivine (as $2Ce_M^{\square} + V_M'' + 3MgO_{surface}$)

This model predicts $[Ce] \propto a_{Ce_2O_3}^{1/2} \cdot [V_M'']^{-1/2} exp\left(-\frac{\Delta v}{2RT}\right) \propto a_{Ce_2O_3}^{1/2} \cdot f_{O2}^{-1/12} exp\left(-\frac{P(3v_{Mg}-2v_{Ce})}{2RT}\right)$.

This is a preprint, the final version is subject to change, of the American Mineralogist (MSA)
Cite as Authors (Year) Title. American Mineralogist, in press.
(DOI will not work until issue is live.) DOI: http://dx.doi.org/10.2138/am-2016-5665

Table 1 Definition of symbols

$\tilde{D}_i^{Y/X}\left(=\frac{\tilde{C}_i^Y}{\tilde{C}_i^X}\right)$	Nernst partition coefficient of element *i* between phase Y and X
$\tilde{C}_i^{Y,X}$	mass fraction of element *i* in a phase Y (X)
$D_i^{Y/X}\left(=\frac{C_i^Y}{C_i^X}\right)$	molar partition coefficient of element *i* between phase Y and X
$C_i^{Y,X}$	molar fraction of element *i* in a phase Y(X)
$K_i^{Y/X}\left(=\frac{a_i^Y}{a_i^X}\right)$	equilibrium constant of element *i* between phase Y and X
$a_i^{Y,X}$	activity of element *i* in a phase Y(X)
μ_X	chemical potential of a phase X
f_X	fugacity of a fluid phase X
r_o	radius of a lattice site at which a trace element is to be placed
r_1	radius of a trace element before placed into the crystal site
$\tilde{r}$	size of the crystal site after the placement of a trace element
$\varepsilon\left(=\frac{\tilde{r}}{r_o}-1\right)$	lattice strain caused by the replacement of a host ion with a trace element
K_1	bulk modulus of a trace element
G_o	shear modulus of the matrix (crystal)
κ	static dielectric constant of the matrix
$\xi\left(=\frac{K_1}{K_1+\frac{4}{3}G_o}\right)$	relative contribution from the trace element and the matrix to strain energy
EEC	effective elastic constant of a site with a trace element
χ^2	measure of the fit of a model to the data
Z_1	electrostatic charge of a trace element
r_{oxy}	radius of oxygen ion
Ar_M''	Ar at the M-site with effective charge of 2-

This is a preprint, the final version is subject to change, of the American Mineralogist (MSA)
Cite as Authors (Year) Title. American Mineralogist, in press.
(DOI will not work until issue is live.) DOI: http://dx.doi.org/10.2138/am-2016-5665

1068 **Table 2** Equations for strain energy of trace element dissolution[*, **]

1069 All Δu are for a defect (for per mole, one should multiply by N_A Avogadro

1070 number).

1071

author	strain energy
Nagasawa (1966)	$\Delta u^{elatsic} = 8\pi r_0^3 \frac{K_o G_o}{K_o+\frac{4}{3}G_o}\left(\frac{r_1}{r_0}-1\right)^2\left[1+\frac{K_o}{K_o+\frac{4}{3}G_o}\left(\frac{r_1}{r_0}-1\right)\right]$ T
Blundy and Wood (1994) (Brice, 1975)	$\Delta u^{elastic} = 6\pi r_0^3 \frac{K_o G_o}{K_o+\frac{G_o}{3}}\left(\frac{r_1}{r_0}-1\right)^2\left[1+\frac{2}{3}\left(\frac{r_1}{r_0}-1\right)\right]$ (T-2)
Karato (this study)	$\Delta u^{elastic} = 6\pi r_0^3 \frac{K_1^2}{K_1+\frac{4}{3}G_0}\left(\frac{r_1}{r_0}-1\right)^2\left[1+\frac{K_1}{K_1+\frac{4}{3}G_0}\left(\frac{r_1}{r_0}-1\right)\right]$ (T-3)

1072

1073 In equations (T-1) and (T-2), I transformed E (Young's modulus) to a combination of

1074 bulk modulus and shear modulus using $E = \frac{9KG}{3K+G}$.

1075 r_o: radius of the site into which a trace element is inserted

1076 r_1: radius of the trace element

1077 K_1: bulk modulus of the trace element

1078 K_o: bulk modulus of the matrix (host crystal)

1079 G_o: shear modulus of the matrix (host crystal)

1080

References

Allan, N.L., Blundy, J.D., Purton, J.A., Lavrentiev, M.Y., and Wood, B.J. (2001) Trace element incorporation in minerals and melts, in: Geiger, C.A. (Ed.), EMU Notes in Mineralogy. Eötvös University Press, Budapest.

Allègre, C.J. (1982) Chemical geodynamics. Tectonophysics, 81, 109-132.

Allègre, C.J., Hofmann, A.W., and O'Nions, K. (1996) The argon constraints on mantle structure. Geophysical Research Letters, 23, 3555-3557.

Allègre, C.J., Staudacher, T., and Sarda, P. (1986/1987) Rare gas systematics: formation of the atmosphere, evolution and structre of the Earth's mantle. Earth and Planetary Science Letters, 81, 127-150.

Allègre, C.J., Staudacher, T., Sarda, P., and Kurz, M. (1983) Constraints on evolution of Earth's mantle from rare gas systematics. Nature, 303, 762-766.

Barrat, J.-L., and Hansen, J.-P. (2003) Basic Concepts for Simple and Complex Liquids. Cambridge University Press, Cambridge.

Blundy, J.D., and Dalton, J. (2000) Experimental comparison of trace element partitioning between clinopyroxene and melt in carbonate and silicate systems, and implications for mantle metasomatism. Contributions to Mineralogy and Petrology, 139, 356-371.

Blundy, J.D., and Wood, B.J. (1994) Prediction of crystal-melt partition coefficients from elastic moduli. Nature, 372, 452-454.

Blundy, J.D., and Wood, B.J. (2003) Partitioning of trace elements between crystals and melts. Earth and Planetary Science Letters, 210, 383-397.

Brice, J.C. (1975) Some thermodynamic aspects of the growth of strained crystals. Journal of Crystal Growth, 28, 249-253.

Broadhurst, C.L., Drake, M.J., Hagee, B.E., and Bernatowicz, T.J. (1992) Solubility and partitioning of Ne, Ar, Kr, and Xe in minerals and synthetic basaltic melts. Geochemica et Cosmochemica Acta, 54, 709-723.

Brodhlot, J.P. (2000) Pressure-induced changes in the compression mechanism of aluminous perovskite in the Earth's mantle. Nature, 407, 620-622.

1110 Brooker, R.A., Du, Z., Blundy, J.D., Kelley, S.P., Allan, N.L., Wood, B.J., Chamorro,
1111 E.M., Wartho, J.-A., and Purton, J.A. (2003) The 'zero charge' partitioning
1112 behaviour of noble gases during mantle melting. Nature, 423, 738-741.
1113 Carroll, M.R., and Stolper, E.M. (1993) Noble gas solubilities in silicate melts and
1114 glasses: New experimental results for argon ad the relationship between solubility
1115 and ionic porosity. Geochimica et Cosmochimica Acta, 57, 5039-5051.
1116 Chakraborty, S. (2010) Diffusion coefficients in olivine, wadsleyite and ringwoodite.
1117 Reviews in Mineralogy and Geochemistry, 72, 603-639.
1118 Chamorro-Perez, E., Gillet, P., Jambon, A., Badro, J., and McMillan, P. (1998) Low
1119 argon solubility in silicate melts at high pressure. Nature, 393, 352-355.
1120 Corgne, A., Liebske, C., Wood, B.J., Rubie, D.C., and Frost, D.J. (2004) Silicate
1121 perovskite-melt partitioning of trace elements and geochemical signature of a deep
1122 perovskite reservoir. Geochimica et Cosmochimica Acta, 69, 485-496.
1123 Dai, L., and Karato, S. (2009) Electrical conductivity of orthopyroxene: Implications for
1124 the water content of the asthenosphere. Proceedings of the Japan Academy, 85,
1125 466-475.
1126 Demouchy, S., Jacobsen, S.D., Gaillard, F., and Stern, C.R. (2006) Rapid magma ascent
1127 recorded by water diffusion profiles in mantle olivine. Geology, 34, 429-432.
1128 Devlal, K., and Gupta, B.R.K. (2007) Equation of state for inert gas solids. Journal of
1129 Physics, Indian Academy of Sciences, 69, 307-312.
1130 Dixon, J.E., Leist, L., Langmuir, J., and Schiling, J.G. (2002) Recycled dehydrated
1131 lithosphere observed in plume-influenced mid-ocean-ridge basalt. Nature, 420,
1132 385-389.
1133 Du, Z., Allan, N.L., Blundy, J.D., Purton, J.A., and Brooker, R.A. (2008) Atomistic
1134 simulation of the mechanisms of noble gas incorporation in minerals. Geochimica
1135 et Cosmochimica Acta, 72, 554-573.
1136 Eshelby, J.D. (1951) The forces on an elastic singularity. Transaction of the Royal
1137 Soceity of London, A244, 87-112.
1138 Eshelby, J.D. (1954) Distortion of a crystal by point imperfections. Journal of Applied
1139 Physics, 25, 255-261.

1140 Eshelby, J.D. (1956) The continuum theory of lattice defects, in: Seitz, F., Turnbull, D.
1141 (Eds.), Solid State Physics. Academic Press, New york, pp. 79-144.
1142 Flynn, C.P. (1972) Point Defects and Diffusion. Oxford University Press, Oxford.
1143 Goldschmidt, V.M. (1937) The principles of distribution of chemical elements in minerals
1144 and rocks. Journal of Chemical Society of London, 140, 655-673.
1145 Guillot, B., and Sarda, P. (2006) The effect of compression on noble gas solubility in
1146 silicate melts and consequences for degassing at mid-ocean ridges. Geochemica et
1147 Cosmochemica Acta, 70, 1215-1230.
1148 Guillot, B., and Sator, N. (2012) Noble gases in high-pressure silicate liquids: A computer
1149 study. Geochimica et Cosmochimica Acta, 80, 51-69.
1150 Hauri, E.H., Gaetani, G.A., and Green, T.H. (2006) Partitioning of water during melting
1151 of the Earth's upper mantle at H_2O-undersaturated conditions. Earth and Planetary
1152 Science Letters, 248, 715-734.
1153 Hazen, R.M., and Finger, L.W. (1979) Bulk modulus-volume relationship for cation-
1154 anion polyhedra. Journal of Geophysical Research, 84, 6723-6728.
1155 Heber, V.S., Brooker, R.A., Kelley, S.P., and Wood, B.J. (2007) Crystal-melt partitioning
1156 of noble gases (helium, neon, argon, krypton, and xenon) for olivine and
1157 clinopyroxene. Geochimica et Cosmochimica Acta, 71, 1041-1061.
1158 Hill, E., Blundy, J.D., and Wood, B.J. (2011) Clinopyroxene-melt trace element
1159 partitioning and the development of a predictive model for HFSE and Sc.
1160 Contributions to Mineralogy and Petrology, 161, 423-438.
1161 Hirose, K., Shimizu, N., Van Westrenen, W., and Fei, Y. (2004) Trace element
1162 partitioning in Earth's lower mantle and implications for geochemical
1163 consequences of partial melting at the core-mantle boundary. Physics of Earth and
1164 Planetary Interiors, 146, 249-260.
1165 Hiyagon, H., and Ozima, M. (1986) Partition of noble gases between olivine and basalt
1166 melt. Geochemica and Cosmochemica Acta, 50, 2045-2057.
1167 Hofmann, A.W. (1997) Mantle geochemistry: the message from oceanic volcanism.
1168 Nature, 385, 219-228.
1169 Jephcoat, A.P. (1998) Rare-gas solids in the Earth's deep interior. Nature, 393, 355-358.

1170 Jing, Z., and Karato, S. (2011) A new approach to the equation of state of silicate melts:
1171 An application of the theory of hard sphere mixtures. Geochimica et
1172 Cosmochimica Acta, 75, 6780-6802.
1173 Jones, J.H. (1995) Experimental trace element partitioning, in: Ahrens, T.J. (Ed.), Rock
1174 Physics and Phase Relations: A Handbook of Physical Constants. American
1175 Goephysical Union, Washington DC, pp. 73-104.
1176 Karato, S. (1977) Rheological Properties of Materials Composing the Earth's Mantle,
1177 Department of Geophysics. University of Tokyo, Tokyo, p. 272.
1178 Karato, S. (1981) Pressure dependence of diffusion in ionic solids. Physics of Earth and
1179 Planetary Interiors, 25, 38-51.
1180 Karato, S. (2008) Deformation of Earth Materials: Introduction to the Rheology of the
1181 Solid Earth. Cambridge University Press, Cambridge.
1182 Karato, S. (2011) Water distribution across the mantle transition zone and its implications
1183 for global material circulation. Earth and Planetary Science Letters, 301, 413-423.
1184 Kittel, C. (1986) Introduction to Solid State Physics, 6th edition ed. John Wiley & Sons,
1185 New York.
1186 Kohlstedt, D.L., Keppler, H., and Rubie, D.C. (1996) Solubility of water in the α, β and γ
1187 phases of $(Mg,Fe)_2SiO_4$. Contributions to Mineralogy and Petrology, 123, 345-
1188 357.
1189 Kohlstedt, D.L., and Mackwell, S.J. (1998) Diffusion of hydrogen and intrinsic point
1190 defects in olivine. Zeitschrift für Phisikalische Chemie, 207, 147-162.
1191 Kröger, F.A., and Vink, H.J. (1956) Relations between the concentrations of
1192 imperfections in crystalline solids, in: Seitz, F., Turnbull, D. (Eds.), Solid State
1193 Physics. Academic Press, San Diego, pp. 307-435.
1194 Lasaga, A.C. (1980) Defect calculations in silicates: olivine. American Mineralogist, 65,
1195 1237-1248.
1196 Lauterbach, S., McCammon, C.A., van Aken, P., Langenhorst, F., and Seifert, F. (2000)
1197 Mössbauer and ELNES spectroscopy of $(Mg,Fe)(Si,Al)O_3$ perovskite: a highly
1198 oxidised component of hte lower mantle. Contributions to Mineralogy and
1199 Petrology, 138, 17-26.

1200 Lee, C.-T.A., Harbert, A., and Leeman, W.P. (2007) Extension of lattice strain theory to
1201 mineral/mineral rare-earth element partitioning: An approach for assessing
1202 disequilbirum and developing internally consistent partition coefficients between
1203 olivine, orthopyroxene, clinopyroxene and basaltic melt. Geochimica et
1204 Cosmochimica Acta, 71, 481-496.
1205 Levien, L., and Prewitt, C.T. (1981) High-pressure structural study of diopside. American
1206 Mineralogist, 66, 315-323.
1207 Maradudin, A.A., Montroll, E.W., Weiss, G.H., and Ipanova, I.P. (1971) Theory of
1208 Lattice Dynamics in the Harmonic Approximation. Academic Press, New York.
1209 Marty, B. (2012) The origins and concentrations of water, carbon, nitrogen and noble
1210 gases on Earth. Earth and Planetary Science Letters, 313/314, 56-66.
1211 Matsui, Y., Onuma, N., Nagasawa, H., Higuchi, H., and Banno, S. (1977) Crystal
1212 structure control in trace element partitioning between crystal and magma. Bull.
1213 Soc. Fr. Mineral. Cristallogr., 100, 315-324.
1214 Mierdel, K., Keppler, H., Smyth, J.R., and Langenhorst, F. (2007) Water solubility in
1215 aluminous orthopyroxene and the origin of Earth's asthenosphere. Science, 315,
1216 364-368.
1217 Mott, N.F., and Littleton, M.J. (1938) Conduction in polar crystals: I. Electrolytic
1218 conduction in solid salts. Transaction of Faraday Society, 34, 485-491.
1219 Mysen, B.O. (1983) The structure of silicate melts. Annual Review of Earth and
1220 Planetary Sciences, 11, 75-97.
1221 Nagasawa, H. (1966) Trace element partition coefficient in ionic crystal. Science, 152,
1222 767-769.
1223 Nakamura, N., and Schmalzried, H. (1983) On the non-stoichiometry and point defects in
1224 olivine. Physics and Chemistry of Minerals, 10, 27-37.
1225 Navrotsky, A. (1999) A lesson from ceramics. Science, 284, 1788-1789.
1226 O'Neill, H.S.C., and Eggins, S.M. (2002) The effect of melt composition on trace element
1227 partitioning: an experimental invetsigation of the activity coefficients fo FeO,
1228 NiO, CoO, MoO_2 and MoO_3 in silicate melt. Chemical Geology, 186, 151-181.

1229 Onuma, N., Higuchi, H., Wakita, H., and Nagasawa, H. (1968) Trace element partitioning
1230 between two pyroxenes and the host lava. Earth and Planetary Science Letters, 5,
1231 47-51.
1232 Ozima, M. (1994) Noble gas state in the mantle. Review of Geophysics, 32, 405-426.
1233 Peslier, A.H., and Luhr, J.F. (2006) Hydrogen loss from olivines in mantle xenoliths from
1234 Simcoe (USA) and Mexico: mafic alkalic magma ascent rates and water budget of
1235 the sub-continental lithosphere. Earth and Planetary Science Letters, 242, 302-
1236 319.
1237 Peslier, A.H., Woodland, A.B., Bell, D.R., and Lazarov, M. (2010) Olivine water contents
1238 in the continental lithosphere and the longivity of cratons. Nature, 467, 78-83.
1239 Pinilla, C., Davis, S.A., Scott, T.B., Allan, N.L., and Blundy, J.D. (2012) Interfacial
1240 storage of noble gases and other trace elements in magmatic systems. Earth and
1241 Planetary Science Letters, 319/320, 287-294.
1242 Purton, J.A., Allan, N.L., Blundy, J.D., and Wasserman, E.A. (1996) Isovalent trace
1243 element partitioning between minerals and melts: A computer simulation study.
1244 Geochimica et Cosmochimica Acta, 60, 4977-4987.
1245 Purton, J.A., Blundy, J.D., and Allan, N.L. (2000) Computer simulation of high
1246 temperature forsterite-melt partitioning. American Mineralogist, 85, 1087-1091.
1247 Sakurai, M., Tsujino, N., Sakuma, H., Kawamura, K., and Takahashi, E. (2014) Effects of
1248 Al content on water partitioning between orthopyroxene and olivine: Implications
1249 for lithosphere-asthenosphere boundary. Earth and Planetary Science Letters, 400,
1250 284-291.
1251 Schmidt, B.C., and Keppler, H. (2002) Experimental evidence for high noble gas
1252 solubilities in silicate melts under mentle pressures. Earth and Planetary Science
1253 Letters, 195, 277-290.
1254 Schmidt, M.W., Connoly, J.A.D., Günther, D., and Bogaerts, M. (2006) Element
1255 partitioning: the role of melt structure and composition. Science, 312, 1646-1650.
1256 Shannon, R.D. (1993) Dielectric polarizabilities of ions in oxides and fluorides. Journal of
1257 Applied Physics, 73, 348-366.
1258 Shcheka, S.S., and Keppler, H. (2012) The origin of the terrestrial noble-gas signature.
1259 Nature, 490, 532-534.

Shibata, T., Takahashi, E., and Matsuda, J.-I. (1998) Solubility of neon, argon, and xenon in binary and ternary silicate systems: A new view on noble gas solubility. Geochimica et Cosmochimica Acta, 62, 1241-1253.

Shibata, T., Takahashi, E., and Ozima, M. (1994) Noble gas partitioning between basaltic melt and olivine crystal at high pressures, in: Matsuda, J.-I. (Ed.), Noble Gas Geochemistry and Cosmochemistry. Terra Scientific Publishing, Tokyo, pp. 343-354.

Spalt, H., Lohstöter, H., and Peisl, H. (1973) Diffuse X-ray scattering from the displacement field of point defects in KBr single crystals. Physica Status Solidi, B56, 469-482.

Tenner, T., Hirschmann, M.M., Withers, A.C., and Hervig, R.L. (2009) Hydrogen partitioning between nominally anhydrous upper mantle minerals and melt between 3 and 5 GPa and applications to hydrous peridotite patial melting. Chemical Geology, 262, 42-56.

Van Orman, J.A., Grove, T.L., and Shimizu, N. (2001) Rare earth element diffusion in diopside: influence of temperature, pressure and ionic radius, and an elastic model for diffusion in silicates. Contributions to Mineralogy and Petrology, 141, 687-703.

Van Orman, J.A., Grove, T.L., and Shimizu, N. (2002) Diffusive fractionation of trace elements during production and transport of melt in Earth's upper mantle. Earth and Planetary Science Letters, 198, 93-112.

Warren, J.M., and Hauri, E.H. (2014) Pyroxenes as tracers of mantle water variations. Journal of Geophysical Research, 119, 1851-1881.

Watson, E.B., Thomas, J.B., and Cherniak, D.J. (2007) ^{40}Ar retention in the terrestrial planets. Nature, 449, 299-304.

Witt-Eickschen, G., and O'Neill, H.S.C. (2005) The effect of temperature on the equilibrium distribution of trace elements between clinopyroxene, orthopyroxene, olivine and spinel in upper mantle peridotite. Chemical Geology, 221, 65-101.

Wood, B.J., and Blundy, J.D. (1997) A predictive model for rare earth element partitioning between clinopyroxene and anhydrous silicate melt. Contributions to Mineralogy and Petrology, 129, 166-181.

1291 Wood, B.J., and Blundy, J.D. (2001) Effect of cation charge on crystal-melt partitioning
1292 of trace elements. Earth and Planetary Science Letters, 188, 59-71.
1293 Wood, B.J., and Blundy, J.D. (2004) Trace element partitioning under crustal and
1294 uppermost mantle conditions: The influence of ionic radius, cation charge,
1295 pressure, and temperature, in: Holland, H.D., Turekian, K.K. (Eds.), Treatise on
1296 Geochemistry. Elsevier, Amsterdam, pp. 395-424.
1297
1298

This is a preprint, the final version is subject to change, of the American Mineralogist (MSA)
Cite as Authors (Year) Title. American Mineralogist, in press.
(DOI will not work until issue is live.) DOI: http://dx.doi.org/10.2138/am-2016-5665

Appendix 1: a modified strain energy model

I consider the elastic strain energy model to calculate the energy change associated with the replacement of an ion in a crystal with another one with different size. In the elastic strain energy model, all materials involved are considered to be elastic media. Accordingly, both the matrix and the trace element are treated as elastic media. Treating a trace element as an elastic medium is a gross simplification. However, by assigning a bulk modulus to the trace element, it is possible to evaluate the influence of "stiffness" of a trace element on the strain energy.

When a crystal is treated as an isotropic elastic medium, the displacement in the matrix and the spherical inclusion is given by (e.g., (Flynn, 1972)),

$$\vec{u}_{0,1} = \left(\frac{A_{0,1}}{r^3} + B_{0,1}\right)\vec{r} \qquad \text{(A-1)}$$

where suffix 0 refers to those for the matrix and 1 to the trace element, and $A_{0,1}$ and $B_{0,1}$ are constants that are to be determined by the boundary conditions. The equation (A-1) has 4 unknowns, $A_{0,1}$ and $B_{0,1}$. The boundary conditions are: (1) $\sigma_{rr}(R) = 0$ (R is the radius the crystal (homogeneous stress caused by pressure is subtracted)), (2) σ_{rr} and u are continuous at the boundary between 1 and 0 ($r = \tilde{r} \equiv (1+\varepsilon) r_0$). Note that the displacement of the boundary, i.e., ε, is also an unknown that must be determined by solving the force balance and displacement continuity equations.

The solution to (A-1) is somewhat tricky to obtain because of the effects of the image force, i.e., the condition $\sigma_{rr}(R) = 0$ (Eshelby, 1951, 1954). We consider first a

This is a preprint, the final version is subject to change, of the American Mineralogist (MSA)
Cite as Authors (Year) Title. American Mineralogist, in press.
(DOI will not work until issue is live.) DOI: http://dx.doi.org/10.2138/am-2016-5665

finite crystal with a finite radius R and consider the proper boundary conditions including the ones at the surface (r=R). Then we let $R \to \infty$. The condition of zero (excess) normal stress at r=R leads to

$$B_0 = \frac{4G_0}{3K_0}\frac{A_0}{R^3}. \qquad \text{(A-2)}$$

Note that although B_0 becomes vanishingly small at $R \to \infty$, it leads to a *finite* volume change of a crystal due to the effect of the image force (Eshelby, 1951, 1954). The volume change of a crystal due to this displacement is

$$\Delta v_c = 4\pi R^2 u(R) = 4\pi A_0 \frac{K_o + \frac{4}{3}G_o}{K_o} = 12\pi A_0 \frac{(1-\nu_0)}{1+\nu_0}. \qquad \text{(A-3)}$$

In addition, there is an explicit volume change caused by the addition of a trace element. Adding the volume change by replacing one atom (ion) with another, the net change in the volume of the whole system is given by

$$\Delta v = \Delta v_c + (v_1 - v_0) = 12\pi A_0 \frac{(1-\nu_0)}{1+\nu_0} + (v_1 - v_0) \qquad \text{(A-4)}$$

where v_1 are the volume of mineral after the trace element is dissolved and v_0 is the volume of the mineral before the trace element dissolution (the volume difference $(v_1 - v_0)$ may correspond to the volume change associated with the formation of point defects). The normal stress at the boundary ($r = \tilde{r} \equiv (1+\varepsilon)r_0$) from the inclusion comes

This is a preprint, the final version is subject to change, of the American Mineralogist (MSA)
Cite as Authors (Year) Title. American Mineralogist, in press.
(DOI will not work until issue is live.) DOI: http://dx.doi.org/10.2138/am-2016-5665

from the initial pressure + displacement. The conditions of continuity of stress and displacement lead to

$$-\frac{4G_0A_0}{\tilde{r}^3}+3K_0B_0=3K_1\left(1-\frac{r_1}{\tilde{r}}\right) \quad \text{(A-5a)}$$

$$\frac{A_0}{\tilde{r}^2}+B_0\tilde{r}=B_1\tilde{r}=\tilde{r}-r_0 \quad \text{(A-5b)}$$

where $K_{0,1}$ are the bulk moduli of the host crystal and the trace element respectively.

From (A-5b), $B_1\tilde{r}=\tilde{r}-r_0=B_1r_0\left(1+\varepsilon\right)=r_0\varepsilon$, so that $B_1=\frac{\varepsilon}{1+\varepsilon}$. Using (A-2) and taking the limit of $R\to\infty$, one obtains $A_0=\varepsilon(1+\varepsilon)^2\,r_0^3$.

Therefore the coefficients in equation (A-1) are given by,

$$A_0=\varepsilon(1+\varepsilon)^2\,r_0^3 \quad \text{(A-6a)}$$

$$A_1=0 \quad \text{(A-6b)}$$

$$B_0=\varepsilon(1+\varepsilon)^2\,\frac{4G_0}{3K_0}\left(\frac{r_0}{R}\right)^3 \quad \text{(A-6c)}$$

$$B_1=\frac{\varepsilon}{1+\varepsilon}. \quad \text{(A-6d)}$$

Inserting these relations into (A-5a) and ignoring the terms containing $\frac{r_0^3}{R^3}$, one obtains

$$\varepsilon=\beta\left(\frac{r_1}{r_0}-1\right) \quad \text{(A-7)}$$

This is a preprint, the final version is subject to change, of the American Mineralogist (MSA)
Cite as Authors (Year) Title. American Mineralogist, in press.
(DOI will not work until issue is live.) DOI: http://dx.doi.org/10.2138/am-2016-5665

with $\beta \equiv \frac{K_1}{K_1+\frac{4}{3}G_o}$. Therefore for a very stiff trace element ($K_1 >> G_0$), $\varepsilon \approx \frac{r_1}{r_0} - 1$ and $\tilde{r} \approx r_1$ whereas for a very soft trace element (e.g., noble gas elements), $K_1 / G_o \ll 1$, so $\varepsilon \approx 0$ and $\tilde{r} \approx r_0$.

The enthalpy associated with the incorporation of trace element is given by

$$\Delta h^{ela} = \Delta u^{ela} + P\Delta \upsilon \qquad \text{(A-8)}$$

where Δu^{ela} is the strain energy and $\Delta \upsilon$ is the volume change of a crystal due to the incorporation of a trace element. From (A-4) and (A-6a), the volume change is given by

$$\Delta \upsilon = 4\pi r_o^3 \left(\frac{r_1}{r_0} - 1\right)\left[1 + \frac{K_o}{K_o+\frac{4}{3}G_o}\left(\frac{r_1}{r_0} - 1\right)\right]^2 + \frac{4\pi}{3} r_0^3 \left(\frac{r_1^3}{r_0^3} - 1\right). \qquad \text{(A-9)}$$

The volume change due to this process is a fraction of atomic volume and is small compared to the volume change associated with vacancy formation.

The strain energy can be calculated as

$$\Delta u^{ela} = 4\pi \left[\int_0^{\tilde{r}} w_1(r) r^2 dr + \lim_{R\to\infty} \int_{\tilde{r}}^{R} w_0(r) r^2 dr\right] \qquad \text{(A-10)}$$

where

$$w_{0,1} = \frac{\lambda_{0,1}}{2}\left(\frac{du_r^{0,1}}{dr} + 2\frac{u_r^{0,1}}{r}\right)^2 + \mu_{0,1}\left[\left(\frac{du_r^{0,1}}{dr}\right)^2 + 2\left(\frac{u_r^{0,1}}{r}\right)^2\right] \qquad \text{(A-11)}$$

This is a preprint, the final version is subject to change, of the American Mineralogist (MSA)
Cite as Authors (Year) Title. American Mineralogist, in press.
(DOI will not work until issue is live.) DOI: http://dx.doi.org/10.2138/am-2016-5665

1383 are the strain energy densities in the host crystal (0) and in the trace element (1)
1384 respectively and where $\lambda_{0,1}, \mu_{0,1}$ are the Lamé constants of the matrix ("0") and the trace
1385 element ("1").

1386 From (A-5), (A-6), (A-7) and (A-11), one gets,

1387

1388 $$w_0 = \frac{9}{2}K_0 B_0^2 + \frac{6G_0 A_0^2}{r^6} = 2A_o^2 \mu_o \left[\frac{4G_o}{K_o}\frac{1}{R^6} + \frac{3}{r^6}\right] \quad \text{(A-12a)}$$

1389 $$w_1 = \frac{9}{2}K_1 B_1^2. \quad \text{(A-12b)}$$

1390

1391 Inserting equations (A-6) and with (A-10),

1392

1393 $$\begin{aligned} \Delta u^{ela} &= 6\pi r_0^3 \varepsilon^2 (1+\varepsilon)\left(K_1 + \tfrac{4}{3}G_0\right) \\ &= 6\pi \frac{K_1^2}{K_1 + \frac{4}{3}G_0} r_0^3 \left(\frac{r_1}{r_0} - 1\right)^2 \left[1 + \frac{K_1}{K_1 + \frac{4}{3}G_0}\left(\frac{r_1}{r_0} - 1\right)\right]. \end{aligned} \quad \text{(A-13)}$$

1394

1395 The equations (A-8), (A-9) and (A-13) give the change in the elastic enthalpy, Δh^{ela},
1396 upon the dissolution of a trace element.

1397

This is a preprint, the final version is subject to change, of the American Mineralogist (MSA)
Cite as Authors (Year) Title. American Mineralogist, in press.
(DOI will not work until issue is live.) DOI: http://dx.doi.org/10.2138/am-2016-5665

Appendix 2: Electrostatic charge and effective elastic constants

Strain energy model is formulated in terms of the size of the site (r_o), the size of a trace element (r_1) and elastic constants of relevant materials (trace element and the host crystal). Comparing a theoretical relationship such as the equations (T-1) through (T-3) with the observed data on element partitioning, one can calculate the effective elastic constant. However, when one does such an exercize, the size of the site at which a peak of partition coefficient is supposedly located does not always agree with the ionic radius of the host ion (e.g., (Blundy and Dalton, 2000)). For instance, in the case of the M2 site of clinopyroxene where trace elements with 3+, 2+ and 1+ charge could go, the estimated r_o from the Onuma diagram agrees well with the ionic radius of the host ion only for trace elements with 2+ charge. The inferred r_o is substantially larger than the ionic radius of the host ion for trace elements with 1+ charge, and it is less than the ionic radius for trace elements with 3+ charge.

This can be attributed to the influence of the charge on the atomic displacement near a point defect. When a point defect such as a vacancy is formed in an ionic crystal, it will create elastic and electric singularities. When a trace element is inserted into that site with an electric charge different from the host ion, it will generate electrostatic force to cause displacement of the ions surrounding it. For a trace element with a charge less (more) than that of the host, the force is repulsive (attractive) and the size of the site will increase (decrease). This explains the systematic shift of r_o with the charge of the trace element.

This effect is largest when the trace element is neutral, i.e., the noble gases.

This is a preprint, the final version is subject to change, of the American Mineralogist (MSA)
Cite as Authors (Year) Title. American Mineralogist, in press.
(DOI will not work until issue is live.) DOI: http://dx.doi.org/10.2138/am-2016-5665

Appendix 3: Some notes on the estimation of $(EEC)_{obs}$

When the solubility of trace elements in a mineral is measured (e.g., the noble gas solubility in bridgmanite (Shcheka and Keppler, 2012)), the elastic strain energy model can be directly compared with the data on the element solubility to calculate the effective elastic constant, *EEC*. In most of trace elements, the available data are the partition coefficients rather than the solubility. In these cases, we need to make an assumption that the concentration of these elements in the melts is independent of the properties of the element. If this assumption is valid, then one can translate the partition coefficient as the solubility, and then compare the results with a model of element solubility (elastic strain energy model)[15].

There is another complication in estimating the *EEC*. When the *EEC* is calculated from the partition coefficients or the solubility, various data for a range of ionic radius (or atomic radius), r_1, are used. This is not trivial because the *EEC* itself likely depends on the size of host ion (r_o) and the size of the trace element (r_1), but the relationship between these parameters and the *EEC* is unknown. Furthermore, even the size of the site, r_o, estimated from the Onuma diagram is sometimes different from the value expected from the ionic radius of the host ion and is treated as an unknown parameter to be determined from the experimental observations (e.g., (Blundy and Dalton, 2000)). Under these circumstances, it is justifiable to obtain a rough estimate of the *EEC* first assuming that it is independent of r_o and r_1, and explore the correlation of the effective elastic constant with other parameters such as r_o and r_1 because the dependence of the *EEC* on these parameters is weak in comparison to the variation in the *EEC*. This can be

[15] This assumption is not valid for the noble gases.

This is a preprint, the final version is subject to change, of the American Mineralogist (MSA)
Cite as Authors (Year) Title. American Mineralogist, in press.
(DOI will not work until issue is live.) DOI: http://dx.doi.org/10.2138/am-2016-5665

seen as follows. The bulk modulus of polyhedron depends on the ionic size as $K_{i,o} \propto Z_{i,o} / \left(r_{i,o} + r_{oxy}\right)^4$ (corrected from (Hazen and Finger, 1979)) where r_{oxy} is the radius of oxygen ion and $Z_{i,o}$ is the electric charge of the trace element or the host ion. When $r_{i,o}$ changes from 0.10 to 0.14 nm, $K_{i,o}$ changes ~30% that is small compared to a variation of the *EEC* among different sites (a factor of ~10-100; (Blundy and Wood, 2003)). Therefore such a procedure of estimating the effective elastic constant can be justified as a first-order approximation.

This is a preprint, the final version is subject to change, of the American Mineralogist (MSA)
Cite as Authors (Year) Title. American Mineralogist, in press.
(DOI will not work until issue is live.) DOI: http://dx.doi.org/10.2138/am-2016-5665

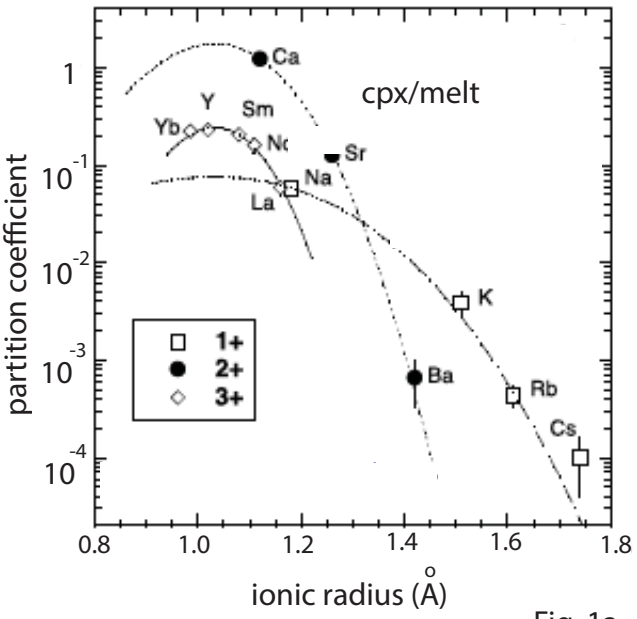

Fig. 1a

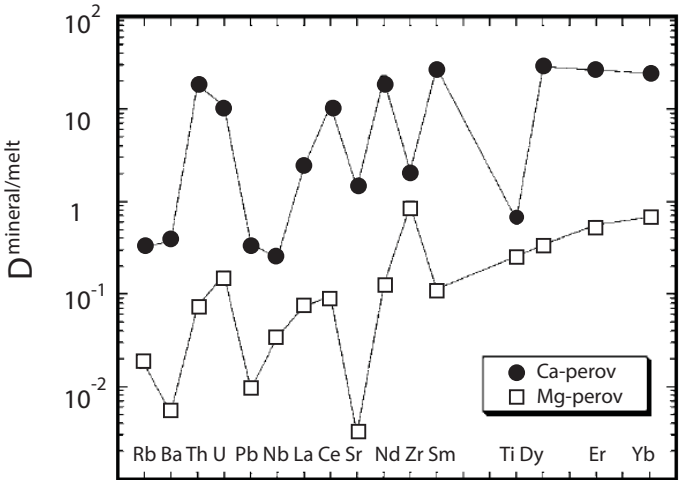

Fig. 1b

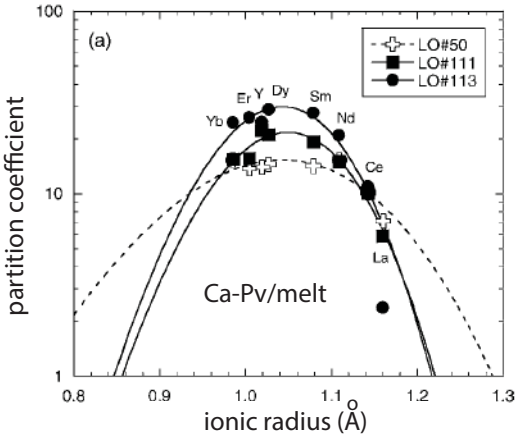

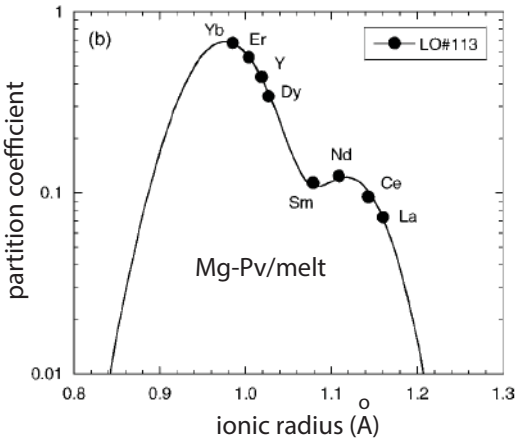

Fig. 1c

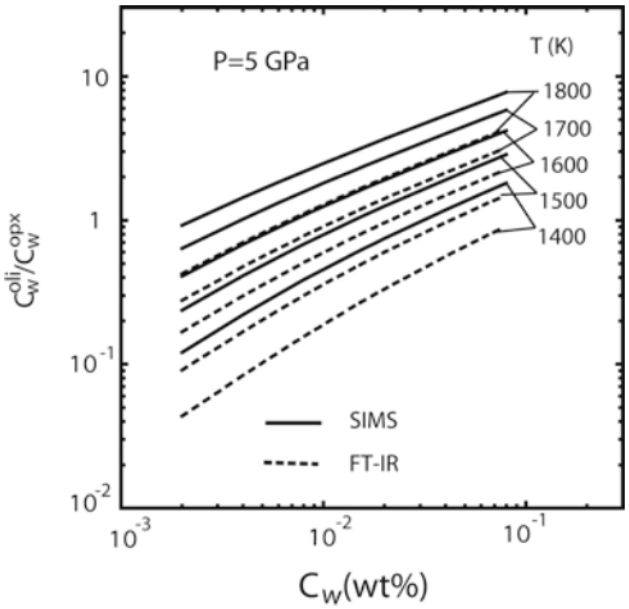

Fig. 1d

This is a preprint, the final version is subject to change, of the American Mineralogist (MSA)
Cite as Authors (Year) Title. American Mineralogist, in press.
(DOI will not work until issue is live.) DOI: http://dx.doi.org/10.2138/am-2016-5665

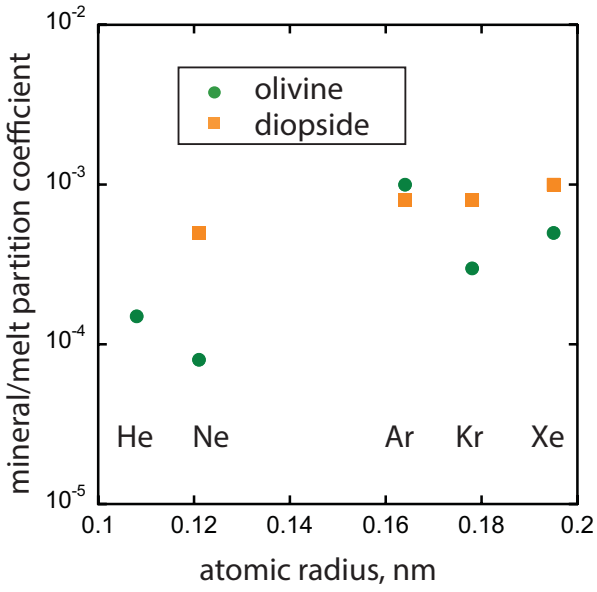

Fig. 1e

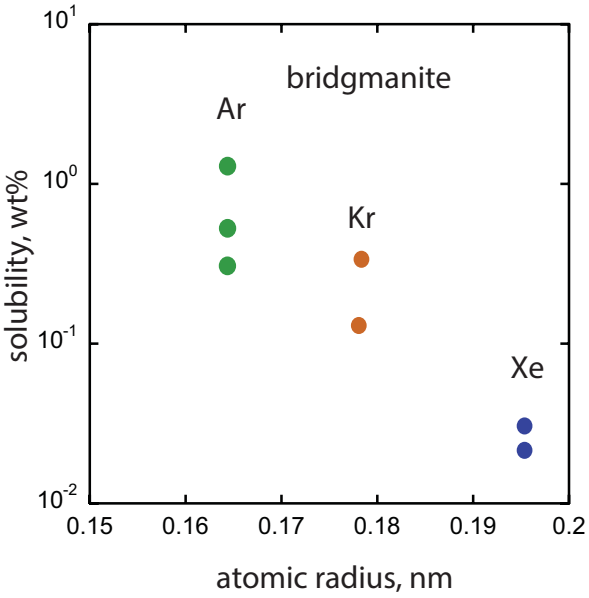

Fig. 1f

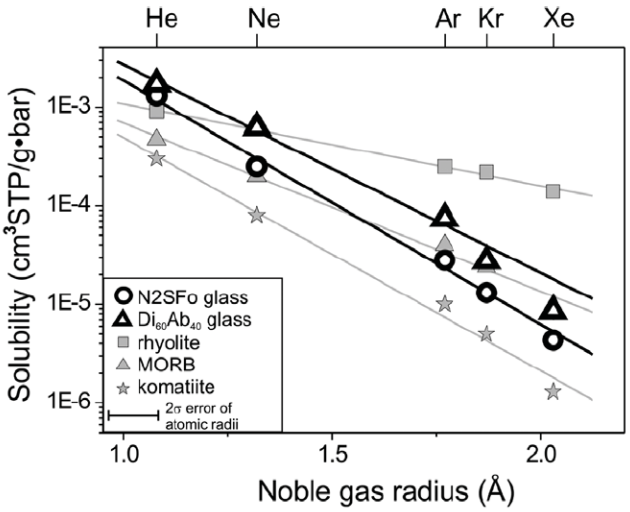

Fig. 1g

This is a preprint, the final version is subject to change, of the American Mineralogist (MSA)
Cite as Authors (Year) Title. American Mineralogist, in press.
(DOI will not work until issue is live.) DOI: http://dx.doi.org/10.2138/am-2016-5665

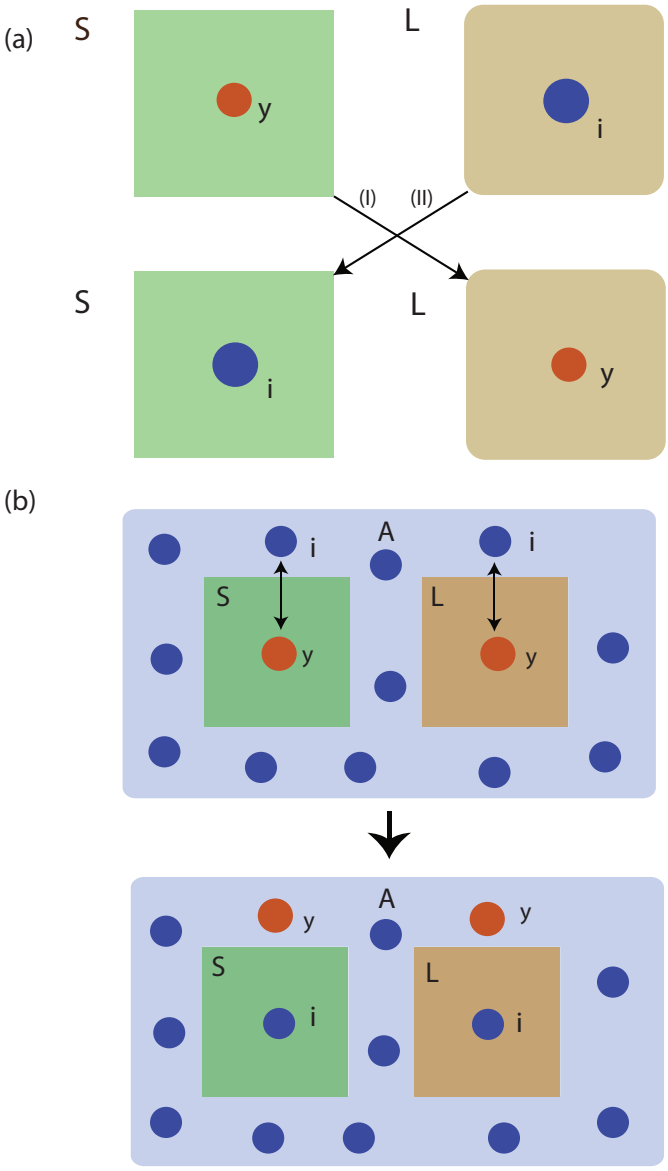

Fig. 2

This is a preprint, the final version is subject to change, of the American Mineralogist (MSA)
Cite as Authors (Year) Title. American Mineralogist, in press.
(DOI will not work until issue is live.) DOI: http://dx.doi.org/10.2138/am-2016-5665

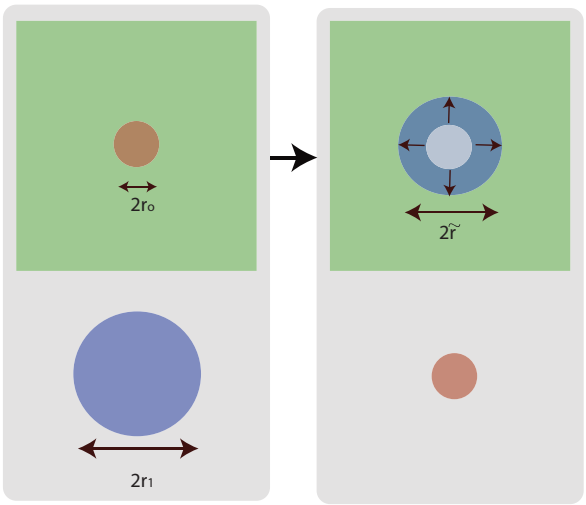

Fig. 3

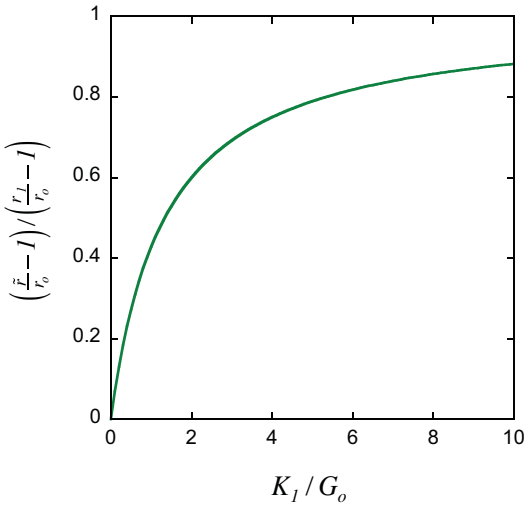

Fig. 4

This is a preprint, the final version is subject to change, of the American Mineralogist (MSA)
Cite as Authors (Year) Title. American Mineralogist, in press.
(DOI will not work until issue is live.) DOI: http://dx.doi.org/10.2138/am-2016-5665

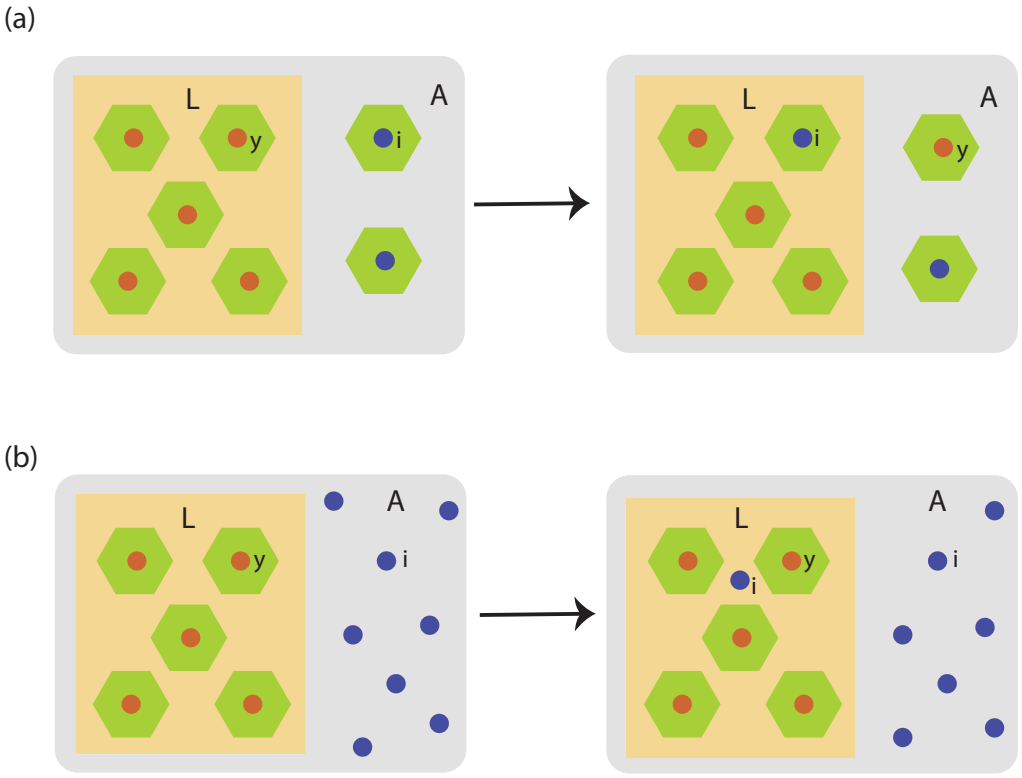

Fig. 5

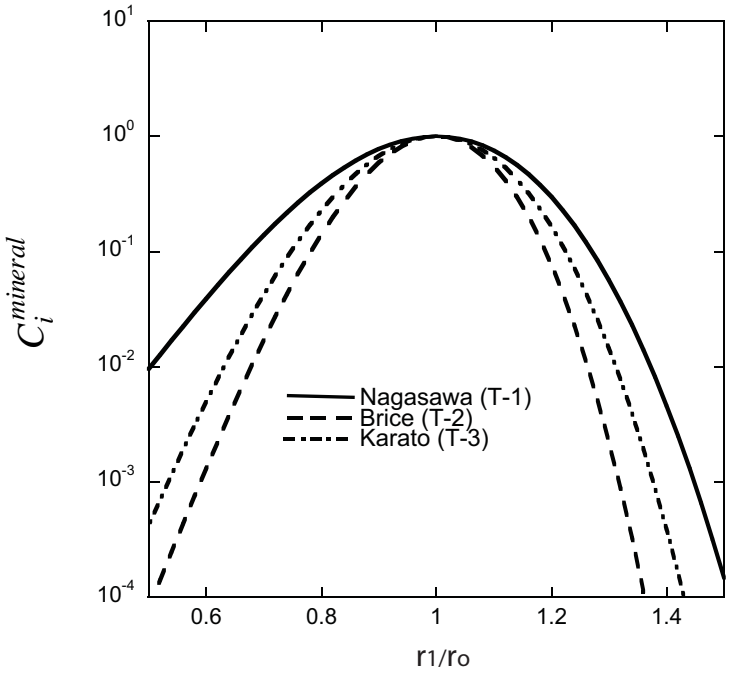

Fig. 6

This is a preprint, the final version is subject to change, of the American Mineralogist (MSA)
Cite as Authors (Year) Title. American Mineralogist, in press.
(DOI will not work until issue is live.) DOI: http://dx.doi.org/10.2138/am-2016-5665

(a)

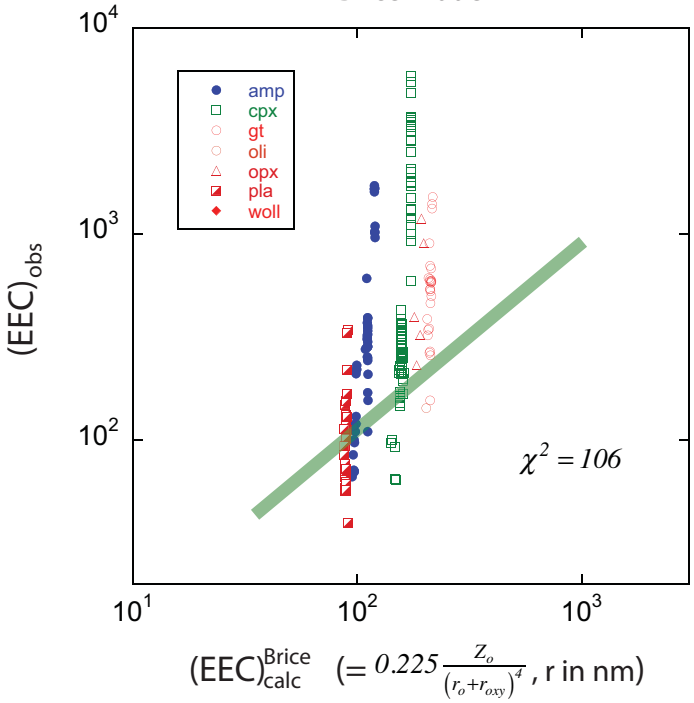

(b)

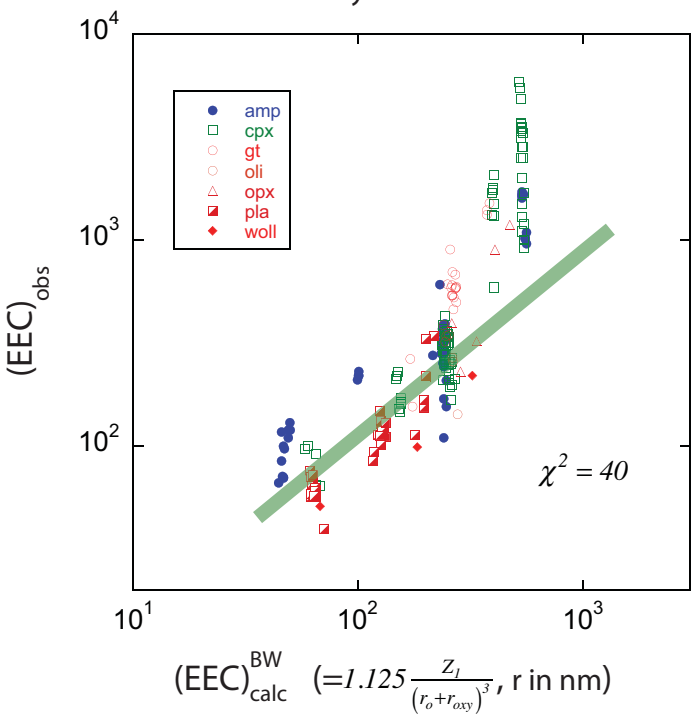

(c)

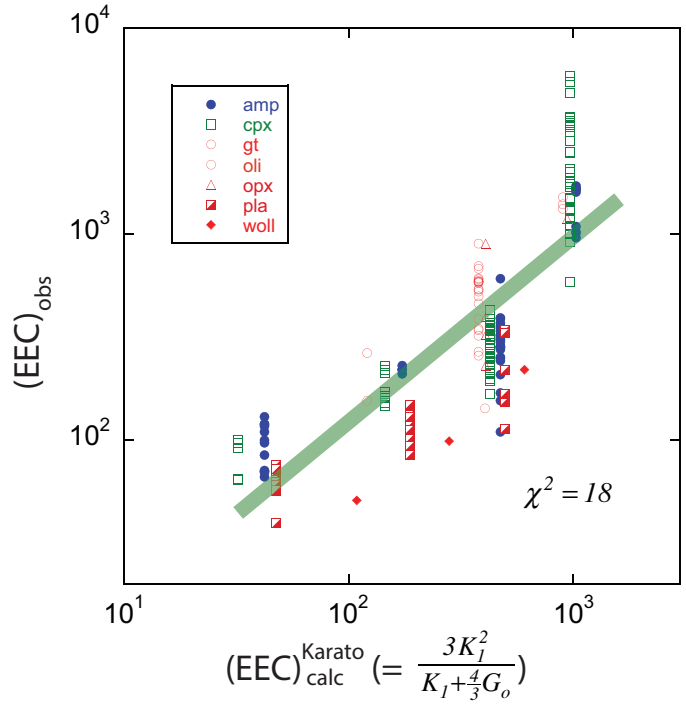

This is a preprint, the final version is subject to change, of the American Mineralogist (MSA)
Cite as Authors (Year) Title. American Mineralogist, in press.
(DOI will not work until issue is live.) DOI: http://dx.doi.org/10.2138/am-2016-5665

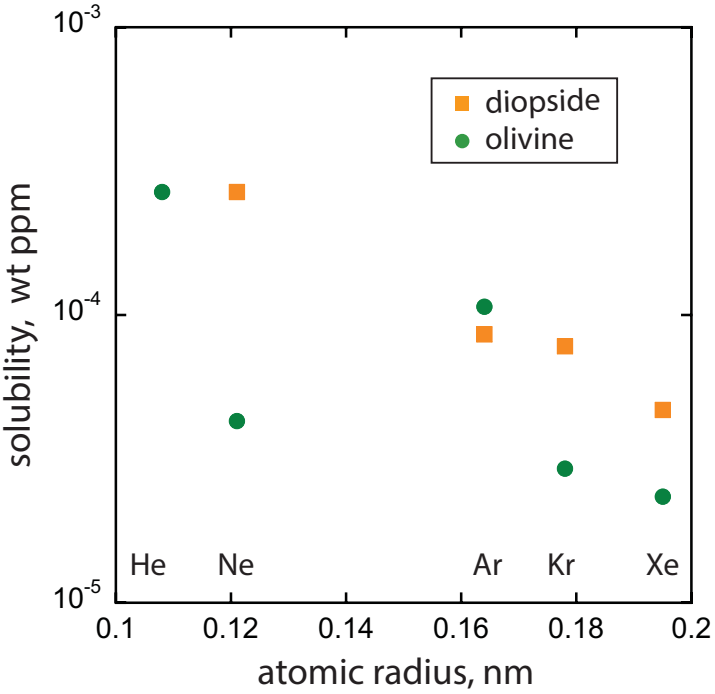

Fig. 8

This is a preprint, the final version is subject to change, of the American Mineralogist (MSA)
Cite as Authors (Year) Title. American Mineralogist, in press.
(DOI will not work until issue is live.) DOI: http://dx.doi.org/10.2138/am-2016-5665

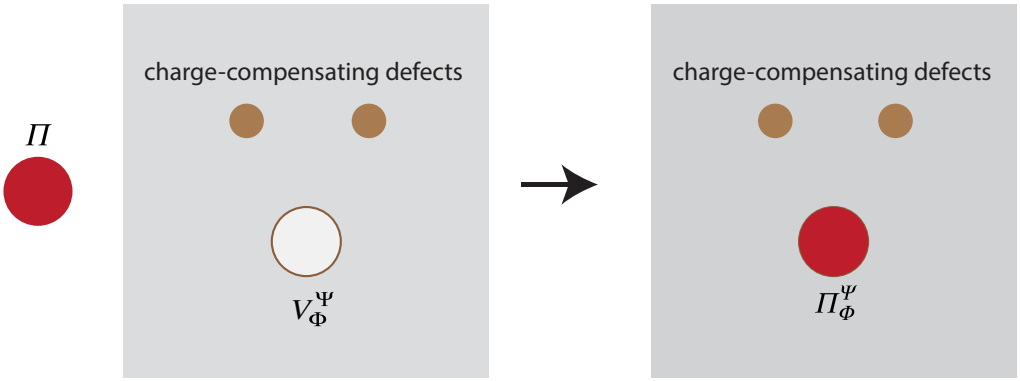

Fig. 9

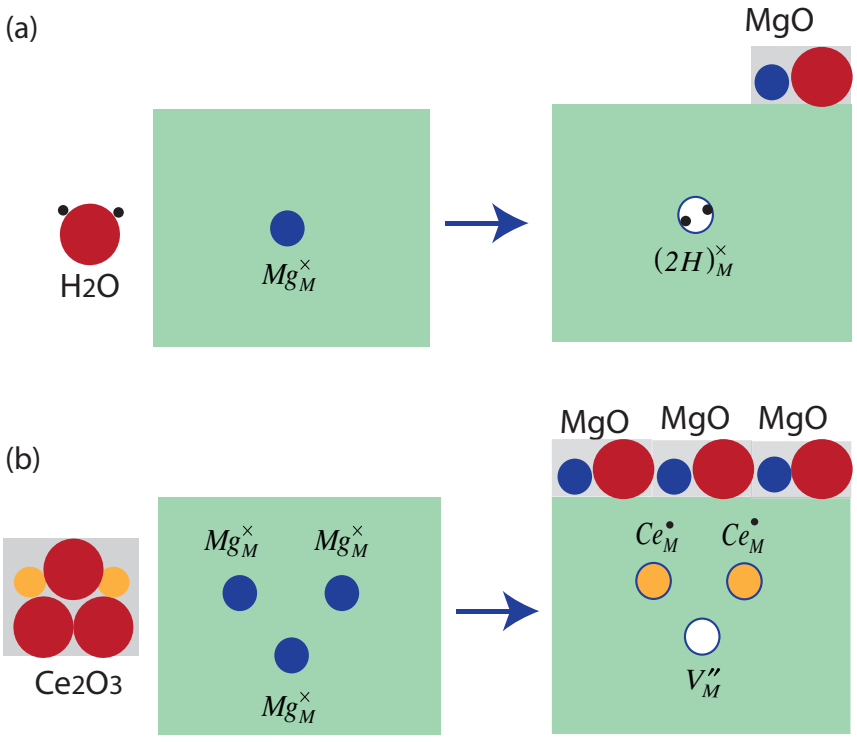

Fig. 10